bioRxiv preprint doi: https://doi.org/10.1101/2019.12.13.875211; this version posted December 13, 2019. The copyright holder for this preprint (which was not certified by peer review) is the author/funder, who has granted bioRxiv a license to display the preprint in perpetuity. It is made available under aCC-BY 4.0 International license.

Anillin/Mid1p interacts with the ECSRT-associated protein Vps4p and mitotic kinases to regulate cytokinesis in fission yeast

Imane M. Rezig[1], Gwyn W. Gould[1,3,4] and Christopher J. McInerny[2,3]

[1] Institute of Molecular, Cell and Systems Biology

[2] School of Life Sciences

Henry Wellcome Laboratory of Cell Biology,
College of Medical, Veterinary and Life Sciences,
Davidson Building,
University of Glasgow,
Glasgow G12 8QQ,
Scotland, United Kingdom

[3] Email: Gwyn.Gould@strath.ac.uk, Chris.McInerny@glasgow.ac.uk

[4] Current address: Strathclyde Institute of Pharmacy and Biomedical Sciences,
University of Strathclyde,
161 Cathedral Street,
Glasgow G4 0RE,
Scotland, United Kingdom

Short title: Interactions of anillin, ESCRT-associated protein Vps4, aurora and polo kinases

bioRxiv preprint doi: https://doi.org/10.1101/2019.12.13.875211; this version posted December 13, 2019. The copyright holder for this preprint (which was not certified by peer review) is the author/funder, who has granted bioRxiv a license to display the preprint in perpetuity. It is made available under aCC-BY 4.0 International license.

Abstract

Cytokinesis is the final stage of the cell cycle which separates cellular constituents to produce two daughter cells. Using *Schizosaccharomyces pombe* we have investigated the role of various classes of proteins involved in this process. Central to these is anillin/Mid1p which forms a ring-like structure at the cell equator that predicts the site of cell separation through septation in fission yeast. Here we demonstrate a direct physical interaction between Mid1p and the endosomal sorting complex required for transport (ESCRT)-associated protein Vps4p. The interaction is essential for cell viability, and Vps4p is required for the correct cellular localization of Mid1p. Furthermore, we show that Mid1p is phosphorylated by the aurora kinase Aurora A, that the interaction of *mid1* and *ark1* genes is essential for cell viability, and that Ark1p is also required for the correct cellular localization of Mid1p. We mapped the sites of phosphorylation of Mid1p by Aurora A and the polo kinase Plk1 and assessed their importance by mutational analysis. Mutational analysis revealed S332, S523 and S531 to be required for Mid1p function and its interaction with Vps4p, Ark1p and Plo1p. Combined our data suggest a physical interaction between Mip1p and Vps4p important for cytokinesis, and identify phosphorylation of Mid1p by aurora and polo kinases as being significant for this process.

Author summary

Replication is a property of all living cells, with cell separation, so-called cytokinesis, the final step in the process. A large number of proteins have been identified that are required for cytokinesis, but in many cases it is not understand how they interact and regulate each other. In this research we have analysed two classes of proteins founds in all eukaryotic cells with central roles in cytokinesis: the endosomal sorting

bioRxiv preprint doi: https://doi.org/10.1101/2019.12.13.875211; this version posted December 13, 2019. The copyright holder for this preprint (which was not certified by peer review) is the author/funder, who has granted bioRxiv a license to display the preprint in perpetuity. It is made available under aCC-BY 4.0 International license.

complex required for transport (ESCRT) proteins and the anillin protein Mid1p. We identify a direct physical interaction between the ESCRT protein Vps4 and anillin/Mid1p, and explore how it regulates cytokinesis. Midp1 activity is shown to controlled by the protein kinase Ark1p by direct phosphorylation, and this phosphorylation is important for Mid1p function. These observations identify new ways in which ESCRT and anillin/Mid1p control cell separation.

Introduction

Much is understood about the control and regulation of the cell division cycle, with many critical cell cycle mechanisms identified being evolutionarily conserved, present across the eukaryotic kingdom. One cell cycle stage that has been increasingly studied is cytokinesis where DNA, organelles and cell constituents are partitioned and allocated to two daughter cells during their physical separation. The fission yeast *Schizosaccharomyces pombe* has proven to be an excellent model organism to study the eukaryotic cell cycle [1]. It is especially useful for studying cytokinesis and cell division as, explicit in its name, it divides by medial fission involving a contractile actomyosin ring leading to the process of cell separation, which is similar to these processes in mammalian cells [2].

A number of proteins have been identified that regulate cytokinesis in fission yeast, including those in a signal transduction pathway named the Septation Initiation Network (SIN) [3]. The SIN proteins form a pathway that facilitates contractile ring constriction and promotes the formation of a medial cell wall-like structure between the two daughter cells, called the septum. Furthermore, SIN components associate with the spindle pole bodies and link mitotic exit with cytokinesis [4]. Sid2p is one regulator of the SIN-cascade of signaling proteins [5]. It terminates the signaling

bioRxiv preprint doi: https://doi.org/10.1101/2019.12.13.875211; this version posted December 13, 2019. The copyright holder for this preprint (which was not certified by peer review) is the author/funder, who has granted bioRxiv a license to display the preprint in perpetuity. It is made available under aCC-BY 4.0 International license.

77 cascade leading to the transition from the spindle pole bodies to the cell division site
78 promoting the onset of cytokinesis [6]. A recent study identified anillin/Mid1p as a
79 substrate for Sid2p and indicated that the phosphorylation of Mid1p facilitates its
80 removal from the cell cortex during the actomyosin contractile ring constriction [7].
81
82 Mid1p forms a ring-like structure at the cell equator that predicts the site of cell
83 separation through the formation of a septum in fission yeast [8,9,10]. In cells
84 containing a chromosomal deletion of the *mid1* gene (*mid1Δ*), a misshaped
85 contractile ring is assembled during anaphase when the SIN pathway becomes
86 active; such observations confirm the important role of Mid1p in directing contractile
87 ring assembly to its correct location [11,12,13].
88
89 Many other groups of proteins have a role in septum formation in *S. pombe*. Amongst
90 these the various classes of ESCRT proteins, including the ESCRT-III regulator
91 Vps4p, were found to be required for septation, suggesting that they have a role in
92 cytokinesis in fission yeast [14,15]. Additional experiments suggested that the
93 ESCRT proteins interacted with established cell cycle regulators including the polo
94 kinase Plo1p, the aurora kinase Ark1p and the CDC14 phosphatase, Clp1p to control
95 these processes [14].
96
97 As a way to further understand the regulation of ESCRT proteins during cytokinesis
98 in fission yeast, we sought to identify other proteins that interact with anillin/Mid1p.
99 Here we describe a direct physical interaction between Vps4p and the anillin Mid1p
100 which is essential for cell viability and for the correct placement of Mid1p. We further
101 show an interaction between Mid1p and the aurora kinase Ark1p which is essential
102 for cell viability and identify phospho-acceptor sites in Mid1p and study their role

bioRxiv preprint doi: https://doi.org/10.1101/2019.12.13.875211; this version posted December 13, 2019. The copyright holder for this preprint (which was not certified by peer review) is the author/funder, who has granted bioRxiv a license to display the preprint in perpetuity. It is made available under aCC-BY 4.0 International license.

using mutagenesis. Collectively, our observations reveal novel mechanisms by which cytokinesis is regulated by different classes of proteins acting through Mid1p.

Results

Genetic and physical interactions between Mid1p and Vps4p in fission yeast

Previously, we identified and characterised the requirement and role of ESCRT proteins for cytokinesis in fission yeast [15]. These experiments also revealed the interaction of ESCRT proteins with three cell cycle regulators, the Polo-like kinase Plo1p, the aurora kinase Ark1p and the CDC14 phosphatase Clp1p. These observations offered a framework by which ESCRT proteins are regulated to control cytokinesis. To further explore ways in which the ESCRT proteins might integrate with other cell cycle regulators to control cytokinesis, we examined their interaction with the anillin Mid1p. Mid1p has a central structural role in cytokinesis, forming equatorial nodes to create an annular shaped structure that determines the position of the division plane [16,13].

We initiated this by searching for genetic interactions between the *mid1* gene and genes encoding ESCRTs and ESCRT-associated proteins. Double mutant fission yeast strains were created containing a chromosomal deletion of *mid1* (*mid1D*) and individual chromosomal deletions of ESCRT genes from Classes E-0 to E-III and *vps4* and searching for synthetic phenotypes. *mid1*Δ was combined with *sst4*Δ (E-0), *sst6*Δ and *vps28*Δ (E-I), *vps36*Δ and *vps25*Δ (EII), *vps20*Δ, *vps32*Δ and *vps2*Δ (E III), and *vps4*Δ [17,15]. In each case double mutants were created which were viable, with no apparent synthetic phenotypes (data not shown). The exception was *mid1*Δ

bioRxiv preprint doi: https://doi.org/10.1101/2019.12.13.875211; this version posted December 13, 2019. The copyright holder for this preprint (which was not certified by peer review) is the author/funder, who has granted bioRxiv a license to display the preprint in perpetuity. It is made available under aCC-BY 4.0 International license.

*vps4*Δ which instead failed to form viable colonies and was synthetically lethal (Fig 1A).

This striking observation demonstrated a genetic interaction between the *mid1* and *vps4* genes, with one explanation that the two encoded proteins interact to control an essential cellular function. To test this hypothesis we expressed and purified a His-tagged version of Vps4p protein from bacteria, using the same method to express and purify three different GST-tagged domains of Mid1p. Full length Mid1p was not purified as it is insoluble under such conditions [16,18].

Full length Mid1p is 920 amino acids in length; the three domains used in pull-down experiments described here encompass the amino acids 1-453 (“N-term”), 452-579 (“Middle”) and 798-920 (“C-term”) [19,18]. Of these three domains, only the C-terminus of amino acids 798-920 was pulled-down by recombinant Vps4p (Fig 1B). This indicates a direct physical interaction between Vps4p and the C-terminus of Mid1p, and that this interaction involved residues 798-920 of Mid1p.

Vps4p is required for the correct cellular distribution of Mid1p

To further understand the interaction between Vps4p and Mid1p we examined the requirement for Vps4p to control the cellular distribution of GFP-tagged Mid1p during the cell cycle. Mid1p distribution has been well characterised and shown to move from the nucleus to the equatorial region to form nodes and a medial ring, that predicts the site of cell cleavage during septation [8].

Wild-type cells showed three patterns of GFP-Mid1p: localization to the nucleus,

bioRxiv preprint doi: https://doi.org/10.1101/2019.12.13.875211; this version posted December 13, 2019. The copyright holder for this preprint (which was not certified by peer review) is the author/funder, who has granted bioRxiv a license to display the preprint in perpetuity. It is made available under aCC-BY 4.0 International license.

cytoplasmic, and equatorial nodes, as previously reported (Fig 2A; [8,5]). By contrast, GFP-Mid1p in *vps4*Δ cells showed strikingly different patterns. Although cytoplasmic GFP-Mid1p was similar to wild-type, additional plasma membrane localization was observed (Fig 2B). In some cells, GFP-Mid1p localized to only one node and the plasma membrane, or localized to three nodes in other cells. The frequencies of these abnormal phenotypes in *vps4*Δ cells were compared with wild-type and showed significant differences (quantified in Fig 2C). Overall, GFP-Mid1p localization was significantly altered by the absence of *vps4*$^{+}$.

These results, in addition to the observation that the *mid1* and *vps4* genes interact genetically, and further that the Mid1p and Vps4p physically interact *in vitro*, suggest that Mid1p and Vps4p coordinate to regulate the *S. pombe* cell cycle.

Genetic and physical interactions between Mid1p and Ark1p in fission yeast

We hypothesized that *mid1* and *ark1* genes interact to accomplish *S. pombe* cytokinesis, as we and others have shown that aurora kinases modulate ESCRT protein function [20,15]. To test this, both genetic and biochemical approaches were taken.

First, a *mid1*Δ strain was crossed with strains containing *ark1*-TS mutations to generate double *mid1*Δ *ark1*-TS mutant strains. The *mid1*Δ *ark1*-TS double mutant failed to form viable colonies (Fig 3A). Such a synthetic lethality indicates a genetic interaction between the *mid1* and *ark1* genes.

bioRxiv preprint doi: https://doi.org/10.1101/2019.12.13.875211; this version posted December 13, 2019. The copyright holder for this preprint (which was not certified by peer review) is the author/funder, who has granted bioRxiv a license to display the preprint in perpetuity. It is made available under aCC-BY 4.0 International license.

As with *mid1* and *vps4* such a genetic interaction might be explained by a physical interaction between Mid1p and Ark1p proteins. Since Ark1p is a protein kinase we tested whether Mid1p can be phosphorylated by aurora kinase, using an *in vitro* phosphorylation approach with recombinant Mid1p domains purified from *E. coli*. These experiments were performed with the human aurora kinases Aurora A, Aurora B, and the human polo kinase Plk1 (Fig 3B). Phosphorylation of both the "N-term" and "Middle" Mid1p domains by Aurora A and Plk1 was detected, but not by Aurora B (Fig 3B; Exp. B and Exp. C). In contrast, no phosphorylation was detected of the "C-term" Mid1p domain by any of the three kinases Aurora A, Aurora B or Plk1 (Fig 3B; Exp. D). These results indicate that, at least *in vitro*, the "N-term" and "Middle" domains of Mid1p interact with and are phosphorylated by both Aurora A and Plk1 kinases, while the "C-term" domain of Mid1p is not phosphorylated by Aurora A, Aurora B or Plk1.

Ark1p is required for the correct cellular distribution of Mid1p

To further analyse the interaction of Ark1p and Mid1p we examined the effect of two different temperature sensitive *ark1* mutants, *ark1*-T11 and *ark1*-T8, on Mid1p distribution in cells (Fig 4).

In *ark1*-T11 cells GFP-Mid1p showed wild-type phenotypes (Fig 4A). But in addition, new localization patterns were apparent, where GFP-Mid1p localization showed nuclear exclusion and appeared to be encircling the nucleus. The frequencies of these phenotypes were quantified and compared to wild-type cells revealing significant differences (Figs 4B). In *ark1*-T8 cells GFP-Mid1p showed new additional localization patterns (Fig 4D). Cells were observed to be round and shorter than the

bioRxiv preprint doi: https://doi.org/10.1101/2019.12.13.875211; this version posted December 13, 2019. The copyright holder for this preprint (which was not certified by peer review) is the author/funder, who has granted bioRxiv a license to display the preprint in perpetuity. It is made available under aCC-BY 4.0 International license.

rod-shaped wild-type cells and GFP-Mid1p localization presented nuclear exclusion and encircled the nucleus. While some cells had one nucleus, others showed two, three, or even four nuclei. The frequencies of these phenotypes were quantified and compared to wild-type cells revealing significant differences (Figs 4E). These data support the hypothesis that Mid1p and Ark1p coordinate to regulate the *S. pombe* cell cycle.

Identification of Mid1p amino acid residues phosphorylated by aurora and polo kinases

To further explore phosphorylation of Mid1p by aurora and polo kinases a mass spectrophotometry approach was used to identify phospho-acceptor sites. The "N-term" and "Middle" domains of Mid1p gel fragments from *in vitro* kinase assay reactions identical to those shown Fig 3B, but with non-labelled ATP, were excised and subjected to nano-scale liquid chromatographic tandem mass spectrometry (nLC-MS/MS) to generate a Mid1p phospho-site map (Fig 5). This analysis identified 35 potential Mid1p residues phosphorylated by either Plk1 or Aurora A kinases (S2 Table). In parallel we examined other published databases on fission yeast phospho-proteomes to refine and confirm the number of Mid1p phospho-sites. Most of these studies used a stable isotope labeling by amino acid in cell culture approach. We selected four studies which studied the *S. pombe* global proteome and identified several Mid1p specific phospho-sites [21-24].

The Mid1p phosphorylation events identified by mass spectrophotometry are summarized in S3 Table, alongside those described by the four published studies. The red highlighted residues represent overlap with the residues identified reported

bioRxiv preprint doi: https://doi.org/10.1101/2019.12.13.875211; this version posted December 13, 2019. The copyright holder for this preprint (which was not certified by peer review) is the author/funder, who has granted bioRxiv a license to display the preprint in perpetuity. It is made available under aCC-BY 4.0 International license.

here. The phospho-sites map shows a total of six potential phospho-sites distributed along the "N-term" and "Middle" Mid1p sequence, five of which were identified in this work, and the sixth was added from the published studies (Fig 5B). These are the serine residues S167, S328, S331, S332, S523 and S531.

To confirm the new phospho-sites identified in Mid1p, *in vitro* phosphorylation experiments involving bacterially expressed phospho-resistant mutant (serine to alanine) forms of the "N-term" and "Middle" domains of Mid1p with Aurora A and Plk1 kinases were completed (Fig 6). These experiments reveled markedly reduced phosphorylation of the Mid1p phospho-resistant mutant S167A by both Aurora A and Plk1 kinases, and S523A by Aurora A alone. These observations support the suggestion that the S167 and S523 residues are phosphorylated by the Aurora A and Plk1 kinases, at least *in vitro*.

Biological relevance of amino acid residues phosphorylated by Ark1p and Plo1p in Mid1p

As another way to examine the role of the phospho-sites identified in Mid1p, we analysed the effect of their mutation *in vivo*. *S. pombe* cells exhibit morphology defects in the absence of Mid1p function. Therefore, we tested the effect of mutations of Mid1p phospho-sites in fission yeast on cell morphology to assay their relevance.

Versions of the *mid1* gene containing phospho-site mutations were generated and integrated in single copy into chromosomal DNA of *S. pombe mid1*Δ cells. Each version of the *mid1* gene had either a phospho-mimetic (S>D) or a phospho-resistant

bioRxiv preprint doi: https://doi.org/10.1101/2019.12.13.875211; this version posted December 13, 2019. The copyright holder for this preprint (which was not certified by peer review) is the author/funder, who has granted bioRxiv a license to display the preprint in perpetuity. It is made available under aCC-BY 4.0 International license.

(S>A) point mutation(s) of the residues S167, S328, S331, S332, S523 or S531 to create a panel of mutant *S. pombe* strains (S1 Fig). Such *mid1* mutations were made both singly and in combination. As a positive control we integrated the wild-type *mid1*$^{+}$ gene into *mid1*Δ cells to create *mid1*Δ pJK148:*mid1*$^{+}$. This resulted in cells that behaved identically to wild-type both on solid medium and in liquid culture (Fig 7 and S1 Fig).

*Mid1p phospho-mutants in mid1*Δ *cells*

Initial experiments examined in *mid1*Δ cells the effect of Mid1p phospho-mimetic or phospho-resistant mutations. Strains were grown on solid medium, with the formation of colonies observed in all cases. In most strains where serine was changed to either alanine or aspartic acid cell morphology appeared similar to wild-type (Fig 7, and data not shown). However, interestingly, *mid1* S332A cells (but not *mid1* S332D) had defects in morphology similar to those observed in *mid1*Δ cells, with slower growth at 25^{o}C (Fig 7). These data indicate a requirement of S332 for Mid1p function.

Furthermore, other phenotypes were revealed when certain Mid1p phospho-mutants were cultured in liquid medium. For example, *mid1* S523A and *mid1* S531A mutants displayed morphology defects (S2 Fig). In contrast, the equivalent phospho-mimetic mutants *mid1* S523D or *mid1* S531D did not.

Mid1p phospho-mutants in ark1-T11 *cells*

To examine the role of Mid1p phosphorylation in its interaction with Ark1p, we crossed the strains containing phospho-mimetic/resistant versions of *mid1* with *ark1*-T11 mutant cells and searched for synthetic phenotypes in double mutants. Viable

bioRxiv preprint doi: https://doi.org/10.1101/2019.12.13.875211; this version posted December 13, 2019. The copyright holder for this preprint (which was not certified by peer review) is the author/funder, who has granted bioRxiv a license to display the preprint in perpetuity. It is made available under aCC-BY 4.0 International license.

276 colonies were observed in all cases with no synthetic phenotypes detected in most
277 double mutants (data not shown). However, *mid1* S523A *ark1*-T11 and *mid1* S531A
278 *ark1*-T11 double mutants showed cell morphology defects when cells were grown in
279 liquid culture more severe than the single mutant strains (S3 Fig). These defects
280 were not observed in the equivalent *mid1* S523D *ark1*-T11 or *mid1* S531D *ark1*-T11
281 double mutants. The cell morphology defects observed in *mid1* S523A *ark1*-T11 and
282 *mid1* S531A *ark1*-T11 double mutants were defined as loss of the rod-like shape of
283 cells. This suggests a role for these two phospho-sites in Mid1p function during the
284 *S. pombe* cell cycle to ensure medial division plane placement, and consequently
285 equal sized and rod-shaped daughter cells.
286
287 *Mid1p phospho-mutants in* plo1-ts35 *cells*
288 To examine the role of Mid1p phosphorylation in its interaction with Plo1p, we
289 crossed strains containing phospho-mimetic/resistant versions of *mid1* with *plo1-ts35*
290 mutant cells and searched for synthetic phenotypes in double mutants. Viable
291 colonies were observed in all cases with no synthetic phenotypes detected for the
292 majority of double mutants (data not shown). However, colony formation on solid
293 medium was slower for *mid1* S332A *plo1-ts35* double mutants, and more severe cell
294 morphology phenotypes were observed, compared to the single mutant strains (data
295 not shown). These defects were not observed in the equivalent *mid1* S332D *plo1-*
296 *ts35* double mutants. Such genetic interactions suggest a link between the regulation
297 of Mid1p and Plo1p.
298
299 *Mid1p phospho-mutants in vps4Δ cells*

bioRxiv preprint doi: https://doi.org/10.1101/2019.12.13.875211; this version posted December 13, 2019. The copyright holder for this preprint (which was not certified by peer review) is the author/funder, who has granted bioRxiv a license to display the preprint in perpetuity. It is made available under aCC-BY 4.0 International license.

To examine the role of Mid1p phosphorylation in its interaction with Vps4p, we crossed strains containing phospho-mimetic/resistant versions of *mid1* with *vps4*Δ mutant cells and searched for synthetic phenotypes in double mutants, Viable colonies were observed in all cases with no synthetic phenotypes detected (data not shown). However, colony formation on solid medium was slower for *mid1* S523D S531D *vps4*Δ double mutants, and more severe cell morphology phenotypes were observed, compared to the single mutant strains. Strikingly, cells had defects in morphology similar to those observed in *mid1*Δ cells (Fig 8). The same serine residues changed to alanine S523A or S531A had no such effect when combined with *vps4*Δ (data not shown). These genetic interactions suggest a link between the regulation of Mid1p by both Vps4p and Ark1p.

Discussion

In fission yeast the Mid1p protein has important roles during cytokinesis during the cell cycle, with anillin homologues having similar roles in higher eukaryotes. These roles centre around its structural role in predicting and controlling the site of cell division in the equatorial region of the cell. Here we have identified new classes of proteins with which Mid1p interacts, and explored the mechanism by which these proteins cooperate and regulate each other and cell growth/morphology.

Mid1p and Vps4p

Genetic and biochemical approaches revealed a direct physical interaction of Mid1p with the ESCRT-associated protein Vps4p. Furthermore, we demonstrated that a chromosomal deletion of the *vps4*$^{+}$ gene caused defects in the cellular localization of GFP-Mid1p. These defects included mis-localization of nodes whereby one node is

bioRxiv preprint doi: https://doi.org/10.1101/2019.12.13.875211; this version posted December 13, 2019. The copyright holder for this preprint (which was not certified by peer review) is the author/funder, who has granted bioRxiv a license to display the preprint in perpetuity. It is made available under aCC-BY 4.0 International license.

randomly positioned, or three nodes were present. This suggests a role of Vps4p in the Mid1p-dependent node localization pathway, which led us to hypothesize that the function of Mid1p is regulated by Vps4p during nodes attachment to the plasma membrane (Fig 9).

Two types of nodes are involved in *S. pombe* actomyosin ring assembly and contraction (Fig 9). Mid1p cortical anchorage first drives the recruitment of cytokinesis proteins, then interactions with myosin filaments causes the condensation of nodes into the actomyosin ring. Mid1p cortical anchorage depends on the PH domain [13] and its potential interaction with Vps4p might stabilize this interaction. Since Vps4p physically interacts with residues within the C-terminal domain of Mid1p, which contains membrane binding motifs, we speculate that Vps4p may facilitate Mid1p cortical anchorage to promote *S. pombe* medial division.

We suggest that a physical interaction between Vps4p and Mid1p regulates Mid1p-dependent node attachment to the plasma membrane to determine the division plane in *S. pombe*, and that this interaction directly or indirectly involves Mid1p PH domain cell cortex anchorage (Fig 9). It is interesting to note that the domain of Mid1p that interacts with Vps4p *in vitro* (Fig 1) contains the PH domain, suggesting that binding of Vps4p to this region may regulate interaction with the cell cortex (Fig 9).

Phosphorylation of Mid1p

Genetic and biochemical approaches revealed a direct physical interaction of Mid1p with the aurora kinase, Ark1p, with Aurora A phosphorylating Mid1p the "N-term" and "Middle" domains. Mapping of the amino acids in Mid1p phosphorylated *in vitro* by Aurora A and Plk1 revealed 35 potential phospho-sites, with some of these sites independently

bioRxiv preprint doi: https://doi.org/10.1101/2019.12.13.875211; this version posted December 13, 2019. The copyright holder for this preprint (which was not certified by peer review) is the author/funder, who has granted bioRxiv a license to display the preprint in perpetuity. It is made available under aCC-BY 4.0 International license.

identified in four *S. pombe* global proteomic studies (Fig 5). Such combined analysis suggested six potential phospho-sites in Mid1p: S167, S328, S331, S332, S523 and S531. Subsequent *in vitro* kinase assay experiments confirmed the *in vitro* phosphorylation of S167, S331 and S523 phospho-sites of Mid1p by Aurora A and Plk1 kinases (Fig 6).

To complement these studies, we examined the effect of mutations of these phospho-sites *in vivo* on cell morphology in wild-type, *ark1-T11, plo1-ts35* and *vps4*Δ *S. pombe* cells. In wild-type cells defective cell morphology phenotypes were observed for the phospho-mimetic mutants S332, S523 and S531 (Fig 7). These were exacerbated when combined with mutations in *ark1, plo1* and *vps4* (Fig 8). Therefore, we conclude that the phosphorylation of these amino acid residues is important for Mid1p function and its interaction with these proteins to regulate cell cycle events. It is tempting to speculate that the interaction of Mid1p and Vps4p is regulated by the activity of Ark1p and/or Plo1p, but it is important to note that the regions of Mid1p phosphorylated by these kinases do not include the binding region for Vps4p. Clearly, phosphorylation in adjacent regions may modulate binding via conformational changes in Mid1p, as regions containing the phospho-acceptor sites have been shown to regulate the interaction of Mid1p with other proteins, including Plo1p and Sid1p. Plo1p phosphorylates residues within the first 100 amino acids of Mid1p to trigger Myosin II recruitment during contractile ring assembly [25]. Later at contractile ring constriction Sid1p phosphorylates Mid1p to facilitate its export from the cell cortex [7]. Future experiments will be aimed at unraveling how the Mid1p interactome is modified both by association with Vps4p and by phosphorylation by mitotic kinases.

bioRxiv preprint doi: https://doi.org/10.1101/2019.12.13.875211; this version posted December 13, 2019. The copyright holder for this preprint (which was not certified by peer review) is the author/funder, who has granted bioRxiv a license to display the preprint in perpetuity. It is made available under aCC-BY 4.0 International license.

Materials and Methods

Yeast media and general techniques

General molecular procedures were performed, with standard methodology and media used for the manipulation of *S. pombe* [26,27]. The yeast strains used in this study are shown in S1 Table. Cells were routinely cultured using liquid or solid complete (YE) or minimal (EMM) medium, at 25^{o}C or 30^{o}C.

DNA constructs

The DNA constructs used in this study are listed in S2 Table. Some were synthesized and cloned by either GenScript or Invitrogen. All constructs were sequenced before use.

Bacterial expression DNA constructs

Four fragments of the *mid1*$^{+}$ gene encoding the amino acids 1-453 “N-terminus”, 452-579 “Middle", 578-799, 798-920 "C-term" [19] were synthesized and cloned into *Bam* HI/*Xho* I of pGEX-4T-1. Full-length *vps4*$^{+}$ was synthesized and cloned into *Nde* I/*Bam* HI of pET-14b. The C-terminal domain of *myo2*$^{+}$ was synthesized and cloned into *Nde* I/*Bam* HI of pET-14b.

mid1 phospho-mimetic/resistant mutants

Eighteen versions of the *mid1* gene with different phospho-mimetic/resistant mutations were synthesized, along with a wild-type *mid1*$^{+}$ control. All had the wild-type *mid1*$^{+}$ promoter in ~1 kbp of DNA upstream of *mid1*$^{+}$ open reading frame, and were each cloned into *Kpn* I/*Sac* I of pJK148. Integration of the pJK148:*mid1* genes (1-19) into *S. pombe mid1*Δ cells was through homologous recombination after

bioRxiv preprint doi: https://doi.org/10.1101/2019.12.13.875211; this version posted December 13, 2019. The copyright holder for this preprint (which was not certified by peer review) is the author/funder, who has granted bioRxiv a license to display the preprint in perpetuity. It is made available under aCC-BY 4.0 International license.

401 linearization of pJK148:*mid1* with *Nde* I in the *leu1*$^{+}$ gene. The resulting panel of
402 phospho-mimetic/resistant mutant strains is listed in S1 Table and S1 Fig.
403
404 *Recombinant protein purification*
405 GST-Mid1p, 6His-Vps4p or 6His-C-term Myo2p plasmids were grown in BL21 *E. coli*
406 until an OD of 0.6-0.8, with protein production induced by adding 1 mM IPTG. Mid1p
407 578-799 was not found to be expressed under these conditions, and so was not used
408 for further experiments.
409
410 Bacterial pellets were produced by centrifugation with cells re-suspended in 20 ml re-
411 suspension buffer with EDTA free protease inhibitors; for GST-Mid1p fusion proteins
412 PBS buffer (137 mM NaCl, 2.7 mM KCl, 10 mM Na_2HPO4 and 1.8 mM KH_2PO4, pH
413 7.4) was used, whereas for 6His-Vps4p, HEPES buffer (25 mM HEPES, 400 mM KCl
414 and 10% (v/v) glycerol, pH 7.4) was used. Cells were then lysed by sonication, where
415 a final concentration of 1 mg ml^{-1} lysozyme was added for cell wall digestion followed
416 by sonication, with 0.1 % (v/v) Triton X-100 added prior to lysis. A clear lysate was
417 produced by centrifugation. GST-tagged fusion proteins were purified using 1ml l^{-1}
418 glutathione beads in PBS buffer, while 6His-tagged Vps4p or C-term Myo2p were
419 purified using 500 µl l^{-1} Ni-NTA beads in HEPES buffer, either for 2 h or overnight at
420 4˚C. Mid1p was eluted from glutathione beads using Reduced glutathione buffer.
421 Vps4p or C-term Myo2p were washed and eluted from Ni-NTA beads using HEPES
422 buffers. Elution was carried out for 2 h at 4˚C. Samples of proteins from each step
423 were subjected to SDS-PAGE to determine elution efficiency.
424
425 *Pull-down experiments*

bioRxiv preprint doi: https://doi.org/10.1101/2019.12.13.875211; this version posted December 13, 2019. The copyright holder for this preprint (which was not certified by peer review) is the author/funder, who has granted bioRxiv a license to display the preprint in perpetuity. It is made available under aCC-BY 4.0 International license.

Pull-down experiments utilized Ni-NTA beads-immobilized bait proteins (6His-Vps4p or 6His- C-term Myo2p) and prey-eluted proteins (GST-Mid1p: “N-terminus”, “Middle” or “C-terminus”) to investigate protein-protein interactions. Bait proteins xx ug were loaded onto Ni-NTA beads by incubation in PBS containing 0.01% (v/v) Triton X-100 for 1 h (4˚C). After loading, the mixture was washed with PBS containing 0.01% (v/v) Triton X-100, and beads were blocked for non-specific binding by incubation in PBS containing 0.2% fish-skin gelatin. The beads mixture was incubated with yy ug prey protein in PBS with 0.01% (v/v) Triton X-100. Subsequently, beads were washed with PBS containing 0.01% (v/v) Triton X-100 three times, 0.5% (v/v) glycerol and 0.2% (w/v) fish skin gelatin three times, and with PBS alone four times. Proteins were eluted from beads by boiling in Laemmli sample buffer (LSB) (75 mM Tris pH 6.8, 12% (w/v) SDS, 60% (v/v) glycerol, 600 mM DTT and 0.6% (w/v) Bromophenol Blue) and samples were subjected to SDS-PAGE.

In vitro *kinase assays*

Assays combined either human Plk1 (0.023 µg/µl), Aurora A (0.01 µg/µl), Aurora B (0.01 µg/µl) and myelin basic protein (MBP; 2.5 µg) (Sigma-Aldrich and Biaffin GmbH) or one of the three Mid1p domains ("N-term", "Middle" or "C-term" 2.5 µg). Kinase, substrate proteins, 1 µCi [γ-^{32}P] ATP, 10 mM ATP and kinase assay buffer (25 mM MOPS, 25 mM $MgCl_2$, 1 mM EDTA and 0.25 mM DTT, pH 7.2) were mixed in a total volume of 20 µl; the reaction was initiated by adding 5 µl ATP cocktail and incubated at 30˚C for 1 h and terminated by the addition of LSB; samples were subjected to SDS-PAGE followed by autoradiography or phospho-imaging. Following detection of *in vitro* phosphorylation signals, mass spectrometric analysis was carried

bioRxiv preprint doi: https://doi.org/10.1101/2019.12.13.875211; this version posted December 13, 2019. The copyright holder for this preprint (which was not certified by peer review) is the author/funder, who has granted bioRxiv a license to display the preprint in perpetuity. It is made available under aCC-BY 4.0 International license.

out by the Dundee FingerPrints Proteomics service (http://proteomics.lifesci.dundee.ac.uk/).

Confocal and light microscopy

Septation and GFP studies were carried out by visualizing *S. pombe* using calcofluor-white stain and fluorescence microscopy, respectively. *S. pombe* cells were cultured in 50 ml YE shaking at 28˚C (25˚C for *ark1*-TS strains) for 18 hours. Cell septa were visualized using bright field and DAPI filters of a Zeiss Axiovert 135 fluorescent microscope equipped with a Zeiss 63X Plan-APOCHROMAT oil-immersion objective lens. GFP-tagged *mid1*$^{+}$ [28] was examined by a He/Ne and Ag laser system of Zeiss LSM microscope using 63X high NA objective lens. Cell images were collected using Zeiss Pascal software and processed using ImageJ, Microsoft PowerPoint and Keynote software. Numerical analysis was completed from three independent experiments where 200-250 cells were counted. Yeast colonies grown on solid medium were imaged using a Zeiss Axioscope microscope and a Sony DSC-75 camera.

Acknowledgements

We thank Anne Paoletti, Tomoko Iwaki and Silke Hauf for sharing fission yeast strains used in this study. We thank Ian Salt for his contribution to this project, both with experimental and practical advice. We acknowledge the following for contributions to experiments: Rianne Cort, Laura Downie, Bethany Hutton, Christina Jack, Jack Goddard, Susan McGill, Mark McLean, Chiamaka Okoli, Elena Pescuma, Liam Pollock, James Provan, John Riddell, Aizhan Shagadatova, Ellen Shercliff, Haoying Wang, and Wandiahyel Yaduma.

bioRxiv preprint doi: https://doi.org/10.1101/2019.12.13.875211; this version posted December 13, 2019. The copyright holder for this preprint (which was not certified by peer review) is the author/funder, who has granted bioRxiv a license to display the preprint in perpetuity. It is made available under aCC-BY 4.0 International license.

References

1. Hoffman C S, Wood V, Fantes P A. An ancient yeast for young geneticists: a primer on the *Schizosaccharomyces pombe* model system. Genetics 2015; 201: 403-423.
2. Willet A H, McDonald N A, Gould K L. Regulation of contractile ring formation and septation in *Schizosaccharomyces pombe*. Curr Opin Microbiol. 2015; 28: 46-52.
3. Simanis V. Pombe's thirteen - control of fission yeast cell division by the septation initiation network. J. Cell Sci. 2015; 128: 1465-1474.
4. Tomlin G C, Morrell J L, Gould K L. The spindle pole body protein Cdc11p links Sid4p to the fission yeast septation initiation network. Mol. Biol. Cell. 2002; 13: 1203-1214.
5. Akamatsu M, Berro J, Pu K M, Tebbs I R, Pollard T D. Cytokinetic nodes in fission yeast arise from two distinct types of nodes that merge during interphase. J. Cell Biol. 2014; 204: 977-988.
6. Sparks C A, Morphew M, McCollum D. Sid2p, a spindle pole body kinase that regulates the onset of cytokinesis. J. Cell. Biol. 1999; 146: 777-790.
7. Willet A H, DeWitt A K, Beckley J R, Clifford D M, Gould K L. NDR kinase Sid2 drives Anillin-like Mid1 from the membrane to promote cytokinesis and medial division site placement. Curr. Biol. 2019; 29: 1055-1063.e2.
8. Paoletti A, Chang F. Analysis of mid1p, a protein required for placement of the cell division site, reveals a link between the nucleus and the cell surface in fission yeast. Mol. Biol. Cell. 2000; 11: 2757-2773.

bioRxiv preprint doi: https://doi.org/10.1101/2019.12.13.875211; this version posted December 13, 2019. The copyright holder for this preprint (which was not certified by peer review) is the author/funder, who has granted bioRxiv a license to display the preprint in perpetuity. It is made available under aCC-BY 4.0 International license.

9. Hachet O, Simanis V. Mid1p/anillin and the septation initiation network orchestrate contractile ring assembly for cytokinesis. Genes Dev. 2008; 22: 3205-3216.
10. Almonacid M, Moseley J B, Janvore J, Mayeux A, Fraisier V, Nurse P, Paoletti A. Spatial control of cytokinesis by Cdr2 kinase and Mid1/Anillin nuclear export. Curr. Biol. 2009; 19: 961-966.
11. Chang F, Woollard A, Nurse P. Isolation and characterization of fission yeast mutants defective in the assembly and placement of the contractile actin ring. J. Cell Sci. 1996; 109: 131-142.
12. Saha S, Pollard T D. Anillin-related protein Mid1p coordinates the assembly of the cytokinetic contractile ring in fission yeast. Mol. Biol. Cell. 2012a; 23: 3982-3992.
13. Sun L, Guan R, Lee I J, Liu Y, Chen M, Wang J, et al. Mechanistic insights into the anchorage of the contractile ring by Anillin and Mid1. Dev. Cell. 2015; 33: 413-426.
14. Bhutta M S, McInerny C J, Gould G W. ESCRT function in cytokinesis: location, dynamics and regulation by mitotic kinases. Int. J. Mol. Sci. 2014a; 15: 21723-21739.
15. Bhutta M S, Roy B, Gould G W, McInerny C J. A complex network of interactions between mitotic kinases, phosphatases and ESCRT proteins regulates septation and membrane trafficking in *S. pombe*. PLoS ONE 2014b; 9: e111789.
16. Rincon S A, Paoletti A. Mid1/anillin and the spatial regulation of cytokinesis in fission yeast. Cytoskeleton 2012; 69: 764-777.

bioRxiv preprint doi: https://doi.org/10.1101/2019.12.13.875211; this version posted December 13, 2019. The copyright holder for this preprint (which was not certified by peer review) is the author/funder, who has granted bioRxiv a license to display the preprint in perpetuity. It is made available under aCC-BY 4.0 International license.

523 17. Iwaki T, Onishi M, Ikeuchi M, Kita A, Sugiura R, Giga-Hama Y, et al. Essential
524 roles of class E Vps proteins for sorting into multivesicular bodies in
525 *Schizosaccharomyces pombe*. Microbiology 2007; 153: 2753-2764.
526 18. Chatterjee M, Pollard T D. The functionally important N-terminal half of fission
527 yeast Mid1p anillin is intrinsically disordered and undergoes phase separation.
528 Biochemistry 2019; 58: 3031-3041.
529 19. Saha S, Pollard T D. Characterization of structural and functional domains of
530 the anillin-related protein Mid1p that contribute to cytokinesis in fission yeast.
531 Mol. Biol. Cell. 2012b; 23: 3993-4007.
532 20. Carlton J G, Caballe A, Agromayor M, Kloc M, Martin-Serrano J. ESCRT-III
533 governs the Aurora B-mediated abscission checkpoint through CHMP4C.
534 Science 2012; 336: 220-225.
535 21. Koch A, Krug K, Pengelley S, Macek B, Hauf S. Mitotic substrates of the
536 kinase Aurora with roles in chromatin regulation identified through quantitative
537 phosphoproteomics of fission yeast. Sci. Signal. 2011; 4: rs6-rs6.
538 22. Carpy A, Krug K, Graf S, Koch A, Popic S, et al. Absolute proteome and
539 phosphoproteome dynamics during the cell cycle of *Schizosaccharomyces*
540 *pombe* (fission yeast). Mol. Cell. Proteomics 2014; 13: 1925-1936.
541 23. Kettenbach A N, Deng L, Wu Y, Baldissard S, Adamo M E, Gerber S A,
542 Moseley J B. Quantitative phosphoproteomics reveals pathways for
543 coordination of cell growth and division by the conserved fission yeast kinase
544 Pom1. Mol. Cell. Proteom. 2015; 14: 1275-1287.
545

bioRxiv preprint doi: https://doi.org/10.1101/2019.12.13.875211; this version posted December 13, 2019. The copyright holder for this preprint (which was not certified by peer review) is the author/funder, who has granted bioRxiv a license to display the preprint in perpetuity. It is made available under aCC-BY 4.0 International license.

24. Swaffer M P, Jones A W, Flynn H R, Snijders A P, Nurse P. Quantitative phosphoproteomics reveals the signaling dynamics of cell-cycle kinases in the fission yeast *Schizosaccharomyces pombe*. Cell Rep. 2018; 24: 503-514.

25. Almonacid M, Celton-Morizur S, Jakubowski J L, Dingli F, Loew D, Mayeux A, et al. Temporal control of contractile ring assembly by Plo1 regulation of Myosin II recruitment by Mid1/Anillin. Curr. Biol. 2011; 21: 473-479.

26. Moreno S, Klar A, Nurse P. Molecular genetic analysis of fission yeast *Schizosaccharomyces pombe*. Methods Enzymol. 1991; 194: 795-823.

27. Rezig I M, Bremner S K, Bhutta M S, Salt I P, Gould G W, McInerny C J. Genetic and cytological methods to study ESCRT cell cycle function in fission yeast. Methods Mol. Biol. 2019; 1998: 239-250.

28. Bähler J, Steever A B, Wheatley S, Wang Y l, Pringle J R, Gould K L, McCollum D. Role of polo kinase and Mid1p in determining the site of cell division in fission yeast. J. Cell Biol. 1998; 143: 1603-1616.

Figure legends

Fig 1. Genetic and physical interactions between *mid1* and *vps4* in fission yeast. (A) Synthetic lethality in *mid1*Δ *vps4*Δ double mutant cells indicates a genetic interaction between the *mid1* and *vps4* genes. Tetrad analysis of h^- *vps4*Δ (*vps4*::*ura4*$^+$) mated with h^+ *mid1*Δ (*dmf1*::*KanMX4*) to identify *vps4*Δ *mid1*Δ double mutants that show a synthetic lethal growth phenotype. Tetrads created by mating the two strains on solid ME medium, four spores dissected and allowed to grow on solid YE medium until colonies formed. Colonies replicated to solid YE+G418/KanMX4 and EMM-ura media and incubated to identify growth phenotypes and double mutants. **(B)** Direct physical interaction between Vps4p and the "C-term"

bioRxiv preprint doi: https://doi.org/10.1101/2019.12.13.875211; this version posted December 13, 2019. The copyright holder for this preprint (which was not certified by peer review) is the author/funder, who has granted bioRxiv a license to display the preprint in perpetuity. It is made available under aCC-BY 4.0 International license.

571 domain of Mid1p. Recombinant GST-tagged (Mid1p domains: "N-term" (aa 1-453),
572 "Middle" (452-579) and "C-term" (793-920)) and 6 His-tagged (Vps4p and "C-term"
573 Myo2p) proteins were expressed in *E. coli* and purified using GST-sepharose beads
574 and Ni-NTA agarose beads, respectively. Exp. A, eluted prey Mid1p domains were
575 added to bait Vps4p bound to Ni-NTA agarose beads: (*) represents physical
576 interaction of Vps4p and Mid1p "C-term" domain. Exp. B, eluted prey Mid1p "N-term"
577 and "Middle" domains were added to bait Myo2p bound to Ni-NTA agarose beads as
578 a positive control: (**) represents physical interaction of Mid1p "N-term" and "Middle"
579 domains with "C-term" domain of Myo2p (left panel). The 14.5 kDa "C-term" Myo2p
580 was not detected in this gel; in a separate experiment (right panel) the detected 14.5
581 kDa "C-term" Myo2p is shown. Asterisks (**) indicate detected physical interactions
582 of Mid1p "N-term" and "Middle" domains with "C-term" domain of Myo2p. Coloured
583 boxes represent predicted proteins: Vps4p purple, Mid1p "N-term" red, Plk1 purple,
584 Mid1p "Middle" green and Mid1p "C-term" dark blue.
585

586 **Fig 2. GFP-Mid1p cellular localization is disrupted in *vps4*Δ cells**. Wild-type (W-
587 T) and *vps4*Δ (*vps4*::*ura*$^{+}$) *S. pombe* strains containing GFP-Mid1p grown at 25˚C in
588 liquid YE medium to mid-exponential phase and visualized by confocal microscopy.
589 **(A)** Key to characterised GFP-Mid1p localization phenotypes. Scale bar, 5 μm. Bright
590 and green fluorescent images of cells (left) and quantitative analysis (right) of GFP-
591 Mid1p localization phenotypes for wild-type (W-T) **(B)** and *vps4*Δ **(C)** cells. Scale bar,
592 10 μm. **(D)** Two-way ANOVA analysis of frequencies of localization phenotypes in
593 *vps4*Δ compared to wild-type (W-T). Asterisks (****) denote *p* values <0.0001
594 indicating significant differences to wild-type. Error bars, SEM.
595

bioRxiv preprint doi: https://doi.org/10.1101/2019.12.13.875211; this version posted December 13, 2019. The copyright holder for this preprint (which was not certified by peer review) is the author/funder, who has granted bioRxiv a license to display the preprint in perpetuity. It is made available under aCC-BY 4.0 International license.

Fig 3. Genetic and physical interactions between *mid1* and *ark1* in fission yeast. (A) Synthetic lethality in *mid1*Δ *ark1*-T11 double mutant cells indicates genetic interaction between *mid1*$^{+}$ and *ark1*$^{+}$ genes. Tetrad analysis of h^{+} *ark1-T11* (*ark1-T11*<<*Kan*^{R}) crossed with h^{-} *mid1*Δ (*mid1*::*ura*$^{+}$) to identify *mid1*Δ *ark1-T11* double mutants that show a synthetic lethal growth phenotype. Tetrads created by mating the two strains on solid ME medium, four spores dissected and allowed to grow on solid YE medium until colonies formed. Colonies replicated to solid YE+G418/KanMX4 and EMM-ura media and incubated to identify growth phenotypes and double mutants. **(B)** Plk1 and Aurora A kinases phosphorylate Mid1p "N-term" and "Middle" domains. Recombinant GST-tagged Mid1p domain proteins "N-term" (aa 1-453), "Middle" (452-579) and "C-term" (798-920) were purified and analysed by *in vitro* phosphorylation assays. In “Exp. A” myelin basic protein (MBP) was a positive control. In “Exp. B”, “Exp. C” and “Exp. D” the "N-term", "Middle" and "C-term" domains of Mid1p were substrates with the kinases Plk1, Aurora A or Aurora B, respectively. Asterisks (*) indicate detected *in vitro* phosphorylation signals. Coloured boxes represent predicted proteins: MBP yellow, Mid1p "N-term" species red, and Mid1p "Middle" species green.

Fig 4. GFP-Mid1p cellular localization is disrupted in *ark1*-T11 and *ark1*-T8 cells. Wild-type (W-T), *ark1*-T11 and *ark1*-T8 *S. pombe* strains containing GFP-Mid1p were grown at 25˚C in liquid YE medium to mid-exponential phase and visualized by confocal microscopy. **(A)** Key to characterised GFP-Mid1p localization phenotypes. Scale bar, 5 μm. Bright and green fluorescent images of cells (left) and quantitative analysis of GFP-Mid1p localisation phenotypes (right) for *ark1*-T11 **(B)** and *ark1*-T8 **(D)**. Scale bar, 10 μm. **(C, E)** Two-way ANOVA analysis of frequencies

bioRxiv preprint doi: https://doi.org/10.1101/2019.12.13.875211; this version posted December 13, 2019. The copyright holder for this preprint (which was not certified by peer review) is the author/funder, who has granted bioRxiv a license to display the preprint in perpetuity. It is made available under aCC-BY 4.0 International license.

621 of localization phenotypes in *ark1*-T11 and *ark1*-T8 compared to wild-type (W-T).
622 Asterisks (****) denote *p* values <0.0001 indicating a significant difference to wild-
623 type. Error bars = SEM.

624

625 **Fig 5. Identification of Mid1p phospho-sites by mass-spectrometry analysis**
626 **(MSA) and published studies. (A)** Mid1p full-length amino acid sequence with "N-
627 term" and "Middle" domains indicated in red and green. Highlighted peptides show
628 35 phosphorylated amino acid residues identified by MSA of *in vitro* phosphorylation
629 reactions for the kinases Plk1 (bold), Aurora A (underlined) or both (bold and
630 underlined). **(B)** Five Mid1p phospho-sites generated from comparison of the 35
631 MSA amino acids with Mid1p phosphorylated amino acids identified in four published
632 proteomic studies [21-24]. Amino acids identified by MSA and four independent
633 studies (pink), MSA and three studies (light blue), and MSA and two studies (dark
634 blue and orange). Asterisk (*) indicates a sixth serine phospho-site at position 531
635 derived from [23] and [24].

636

637 **Fig 6. Reduced *in vitro* phosphorylation of Mid1p "N-term and "Middle"**
638 **phospho-resistant mutants by Plk1 and Aurora A kinases.** Recombinant GST-
639 tagged Mid1p "N-term" **(A)** and "Middle" **(B)** domains phospho-resistant mutants
640 were expressed and purified in *E. coli*. Proteins subjected to *in vitro* phosphorylation
641 experiments with Aurora A (Exp. A) or Plk1 (Exp. B) kinases. Asterisks (* and **)
642 indicate wild-type Mid1p "N-term" and Mid1p "Middle" recombinant proteins used as
643 positive controls. Coloured boxes represent predicted proteins: MBP yellow, Mid1p
644 "N-term" species red, Plk1 purple, and all Mid1p "Middle"-related species green.
645 "Multiple" indicates mutations in all four phospho-sites.

bioRxiv preprint doi: https://doi.org/10.1101/2019.12.13.875211; this version posted December 13, 2019. The copyright holder for this preprint (which was not certified by peer review) is the author/funder, who has granted bioRxiv a license to display the preprint in perpetuity. It is made available under aCC-BY 4.0 International license.

Fig 7. The S332 phospho-site is required for Mid1p function. Three phospho-resistant *mid1* mutant strains *mid1* S332A, *mid1* S167A S328A S331A S332A, and *mid1* S167A S328A S331A S332A S523A S531A, and the three phospho-mimetic mutants *mid1* mutant strains S332D, *mid1* S167D S328D S331D S332D, and *mid1* S167D S328D S331D S332D S523D S531D streaked to single colonies on solid YE at 25˚C to compare growth rates **(A)** and colony morphology **(B)**. Controls: *mid1*Δ and wild-type (W-T) cells. Scale bar, 10 μm.

Fig 8. The Mid1p S523 and S531 phospho-sites regulate its interaction with Vps4p. Strains streaked to single colonies on solid YE medium and grown at 25˚ to compare growth rates and colony morphology. Controls: *vps4*Δ and wild-type (W-T) cells. Scale bar, 10 μm.

Fig 9. Interaction of Mid1p and Vps4p to regulate *S. pombe* septation. (A) Schematic representation of Mid1p localization during *S. pombe* cell cycle stages. CR = contractile ring. **(B)** Mid1p is phosphorylated by Plo1p to promote mitotic entry, during which Rng2p and other proteins interact with the N-terminal domain of Mid1p. **(C)** In mitosis, Mid1p forms nodes which are attached to the plasma membrane via the lipid binding motifs present within the Mid1p C-terminal domain. Green box represent the overall structure of Mid1p C-terminal region (aa 579-920) containing: the C2 domain (cyan), the connector domain (red) and the PH domain (yellow); dotted lines represent the lipid binding loop. Structure adapted from [13]. The Vps4p interaction with the C-terminal domain of Mid1p potentially regulates this process.

bioRxiv preprint doi: https://doi.org/10.1101/2019.12.13.875211; this version posted December 13, 2019. The copyright holder for this preprint (which was not certified by peer review) is the author/funder, who has granted bioRxiv a license to display the preprint in perpetuity. It is made available under aCC-BY 4.0 International license.

671 **S1 Fig. Summary of Mid1p phospho-mimetic/resistant fission yeast mutant**
672 **strains used in this study.** Top Panel: full length Mid1p with S167, S328, S331,
673 S332, S523 and S531 phospho-sites indicated. Lower Panel: summary of single or
674 combinatorial ("Multi") phospho-mimetic or phospho-resistant mutations of the *mid1*
675 gene, to generate eighteen versions integrated into *mid1*Δ cells, with each yeast
676 strain given a "GG" lab collection number.
677
678 **S2 Fig. *mid1* phospho-resistant/mimetic mutants reveal cell division**
679 **phenotypes.** Wild-type (W-T), *mid1*Δ, *mid1Δ* pJK148:*mid1*$^{+}$, *mid1Δ*
680 pJK148:*mid1*S523A, *mid1Δ* pJK148:*mid1*S523D, *mid1Δ* pJK148:*mid1*S531A, *mid1Δ*
681 pJK148:*mid1*S531D, *mid1Δ* pJK148:*mid1*S523A S531A and *mid1Δ*
682 pJK148:*mid1*S523D S531D strains grown at 25˚C in liquid YE medium to mid-
683 exponential phase. Cells visualized by confocal microscopy under bright field. Scale
684 bar, 10 μm. Characterised cell morphology phenotypes indicated by red arrows. **(A)**
685 Two-way ANOVA analysis of frequencies of localization phenotypes in wild-type (W-
686 T), *mid1Δ* and *mid1Δ* pJK148:*mid1*$^{+}$ cells. **(B)** Key to characterised cell morphology
687 phenotypes. Scale bar, 5 μm. **(C-E)** Two-way ANOVA analysis of frequencies of
688 localization phenotypes of *mid1* phospho-resistant/mimetic mutants. Asterisks (****)
689 denote *p* values <0.0001 indicating significant difference to wild-type. Error bars =
690 SEM.
691
692 **S3 Fig. *mid1* phospho-resistant/mimetic *ark1*-T11 double mutants reveal cell**
693 **division phenotypes.** *ark1*-T11, *mid1Δ ark1*-T11 pJK148:*mid1*$^{+}$, *mid1Δ ark1*-T11
694 pJK148:*mid1*S523A, *mid1Δ ark1*-T11 pJK148:*mid1*S523D, *mid1Δ ark1*-T11
695 pJK148:*mid1*S531A, *mid1Δ ark1*-T11 pJK148:*mid1*S531D, *mid1Δ ark1*-T11

bioRxiv preprint doi: https://doi.org/10.1101/2019.12.13.875211; this version posted December 13, 2019. The copyright holder for this preprint (which was not certified by peer review) is the author/funder, who has granted bioRxiv a license to display the preprint in perpetuity. It is made available under aCC-BY 4.0 International license.

696 pJK148:*mid1*S523A S531A and *mid1Δ ark1*-T11 pJK148:*mid1*S523D S531D strains
697 grown at 25˚C in liquid YE medium to mid-exponential phase. Cells visualized by
698 confocal microscopy under bright field. Scale bar, 10 µm. Characterised cell
699 morphology phenotypes indicated by red arrows. **(A)** Two-way ANOVA analysis of
700 frequencies of localization phenotypes in wild-type (W-T), *ark1*-T11 and *mid1*Δ
701 pJK148:*mid1*$^{+}$ *ark1*-T11 cells. (**B)** Key to characterised cell morphology phenotypes.
702 Scale bar, 5 µm. **(C-E)** Two-way ANOVA analysis of frequencies of localization
703 phenotypes in wild-type (W-T), *mid1* phospho-resistant/mimetic and *ark1*-T11 cells.
704 Asterisks (****) denote *p* values <0.0001 indicating significant difference to wild-type.
705 Error bars = SEM.

bioRxiv preprint doi: https://doi.org/10.1101/2019.12.13.875211; this version posted December 13, 2019. The copyright holder for this preprint (which was not certified by peer review) is the author/funder, who has granted bioRxiv a license to display the preprint in perpetuity. It is made available under aCC-BY 4.0 International license.

(A)

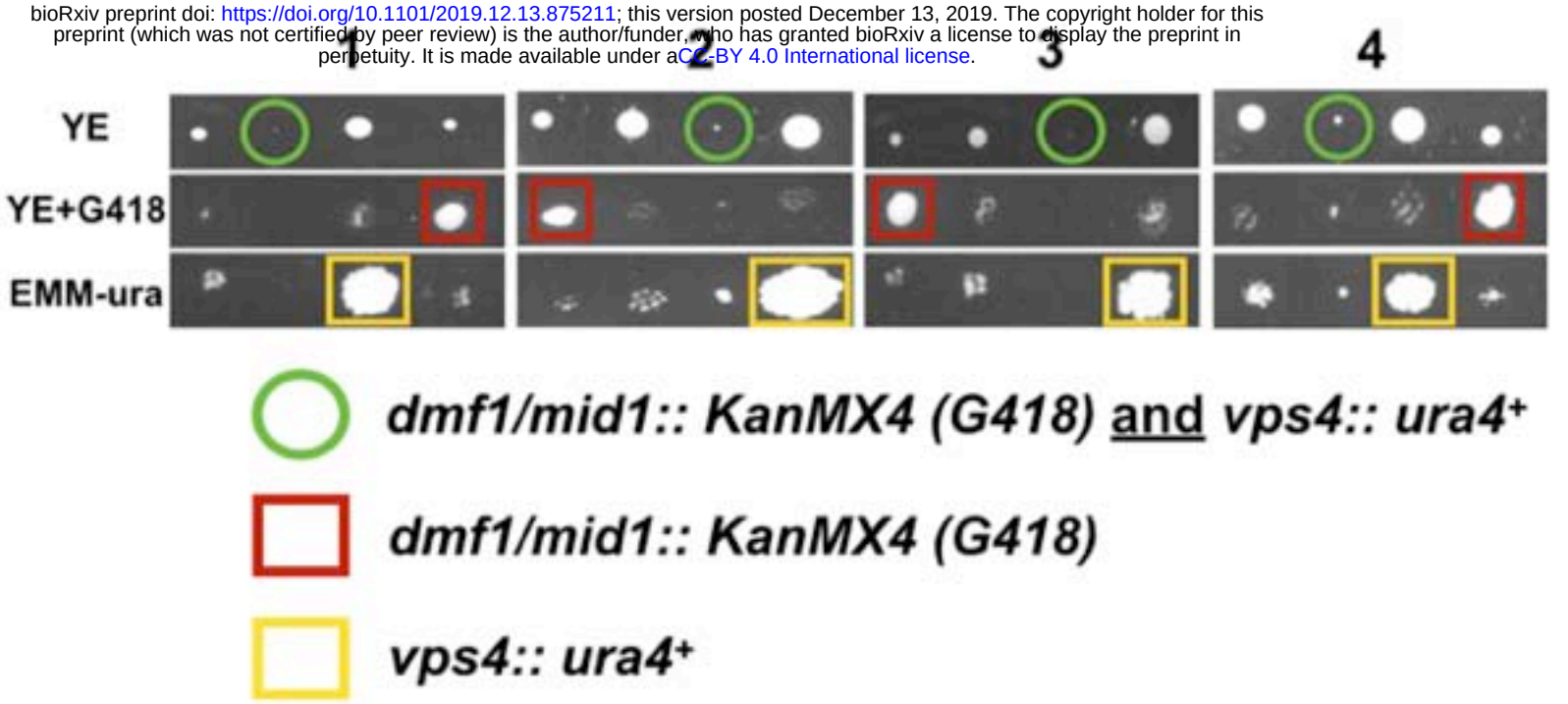

(B)

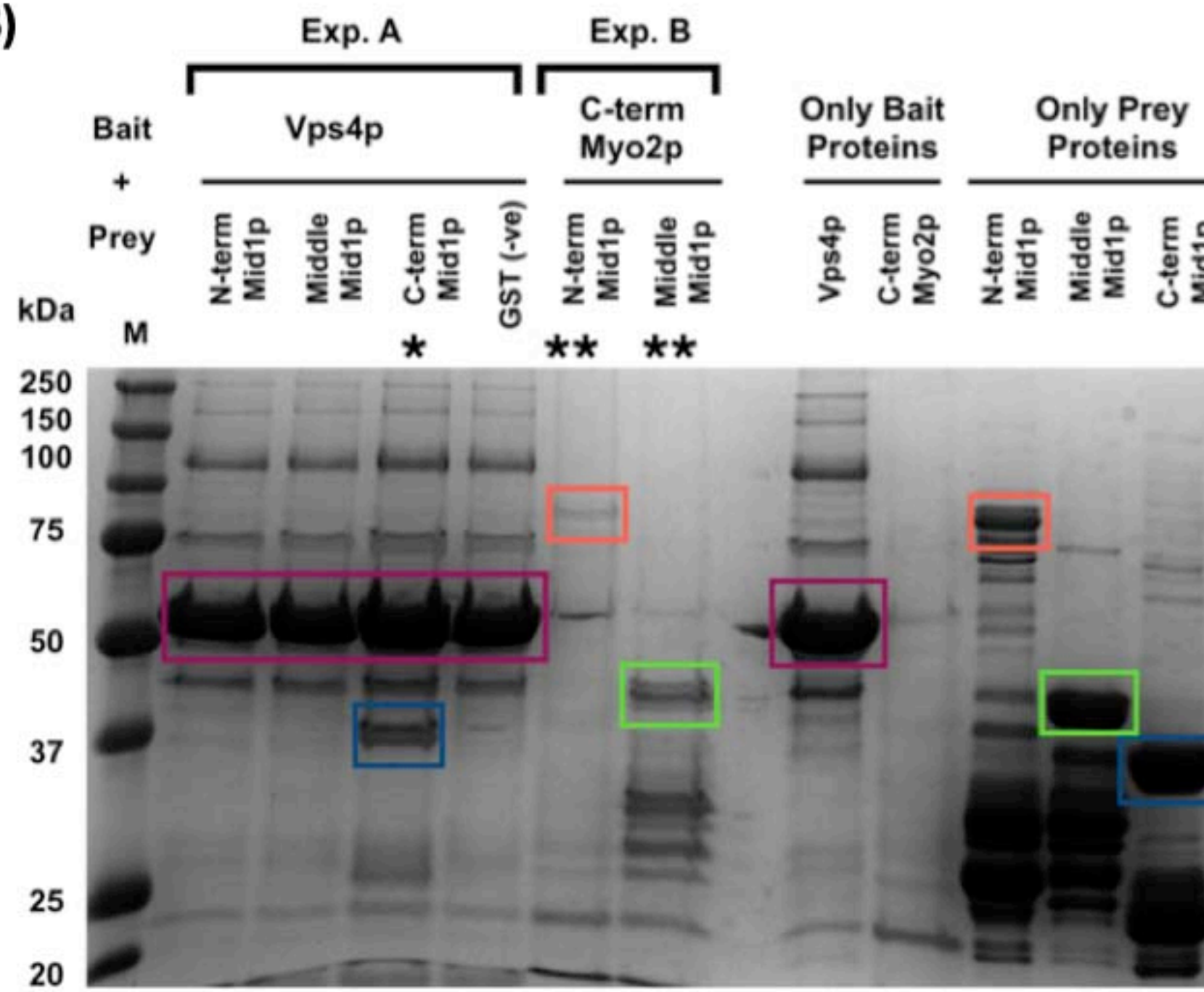

preprint (which was not certified by peer review) is the author/funder, who has granted bioRxiv a license to display the preprint in perpetuity. It is made available under aCC-BY 4.0 International license.

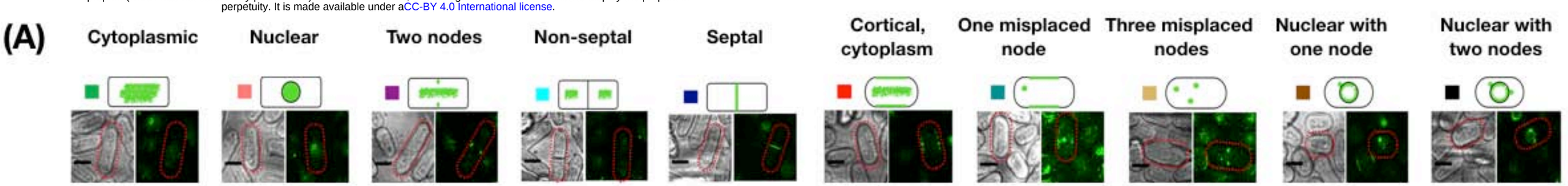

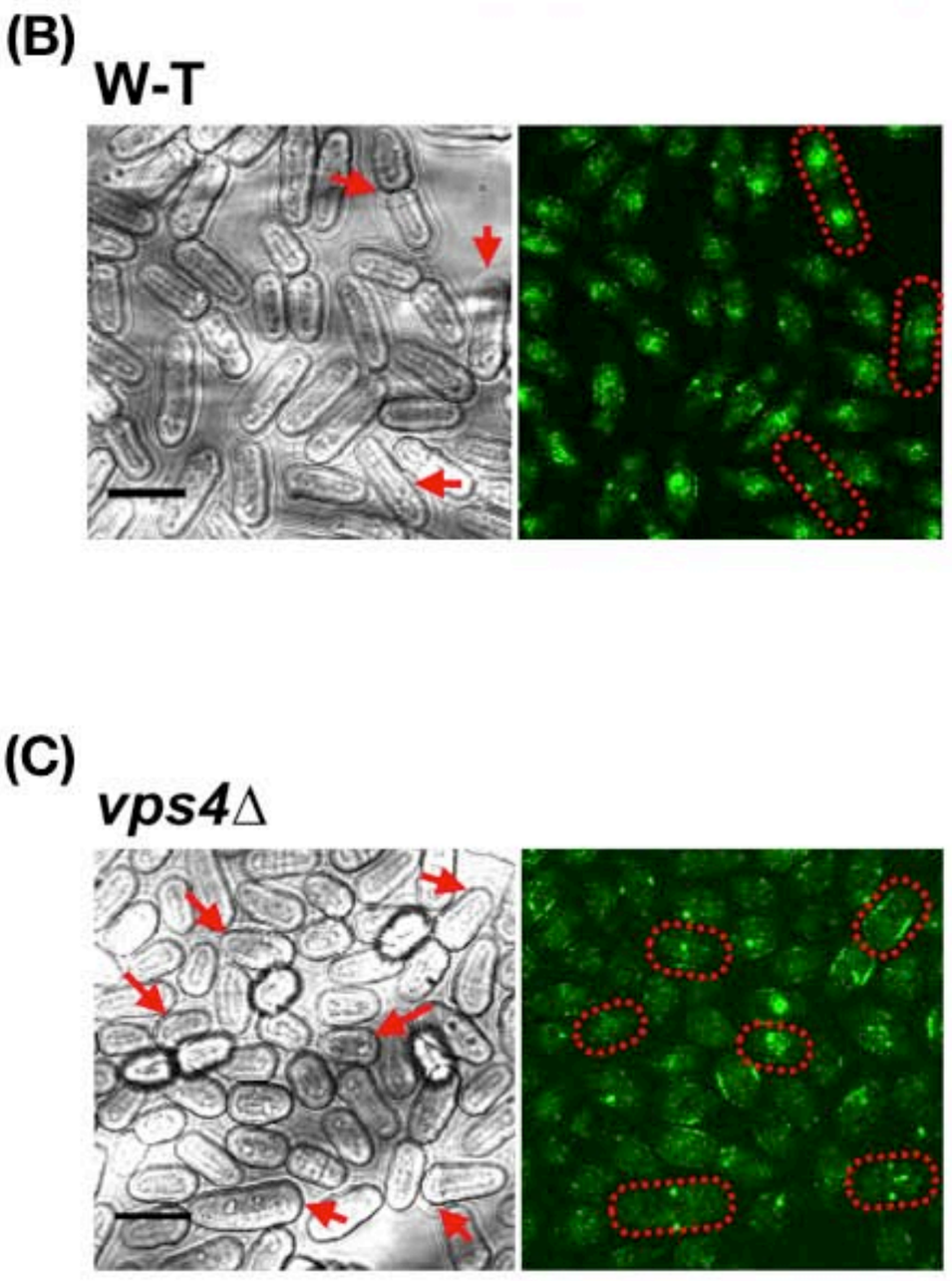

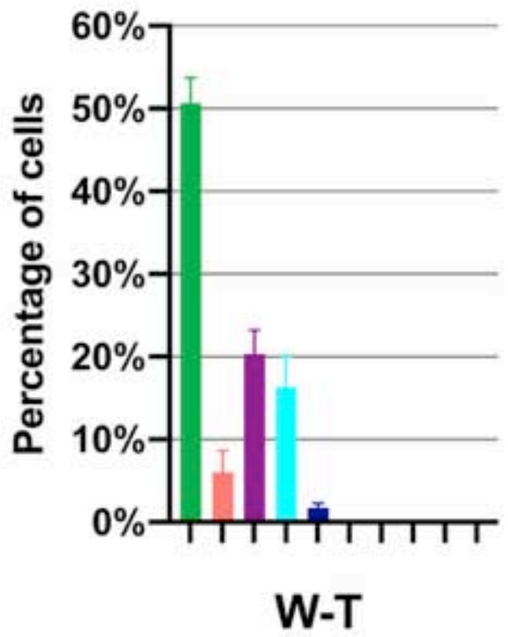

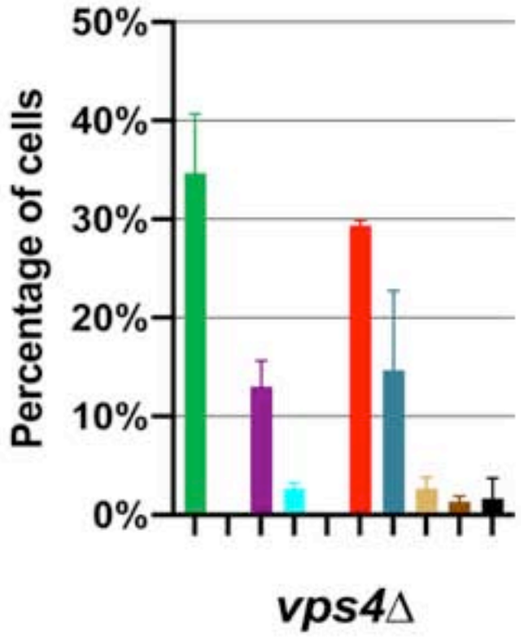

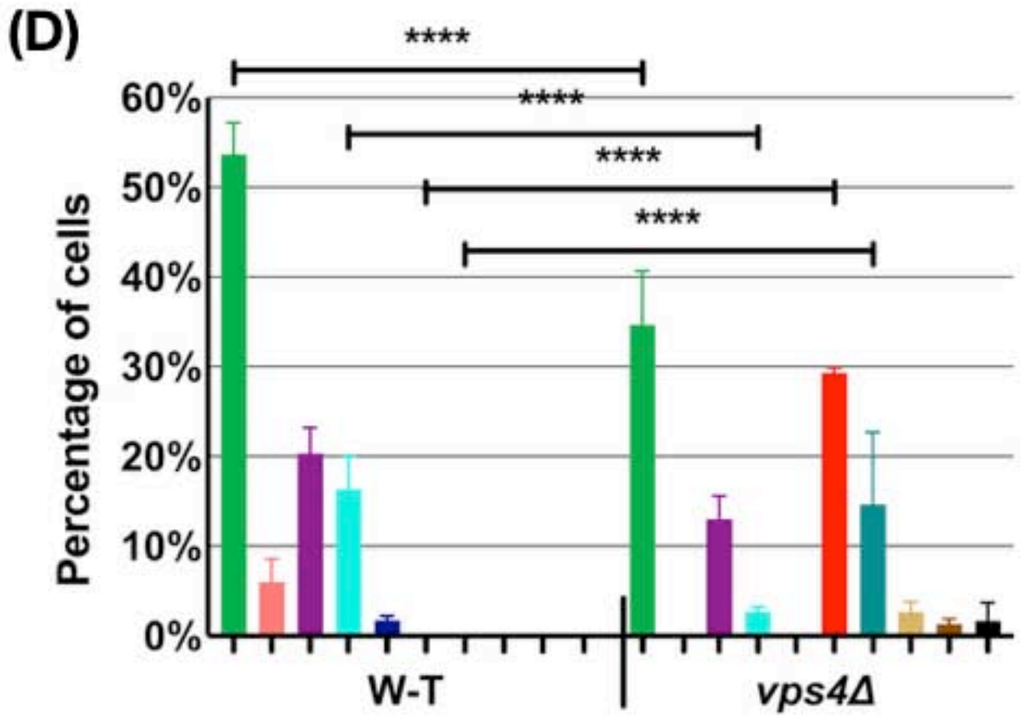

bioRxiv preprint doi: https://doi.org/10.1101/2019.12.13.875211; this version posted December 13, 2019. The copyright holder for this preprint (which was not certified by peer review) is the author/funder, who has granted bioRxiv a license to display the preprint in perpetuity. It is made available under aCC-BY 4.0 International license.

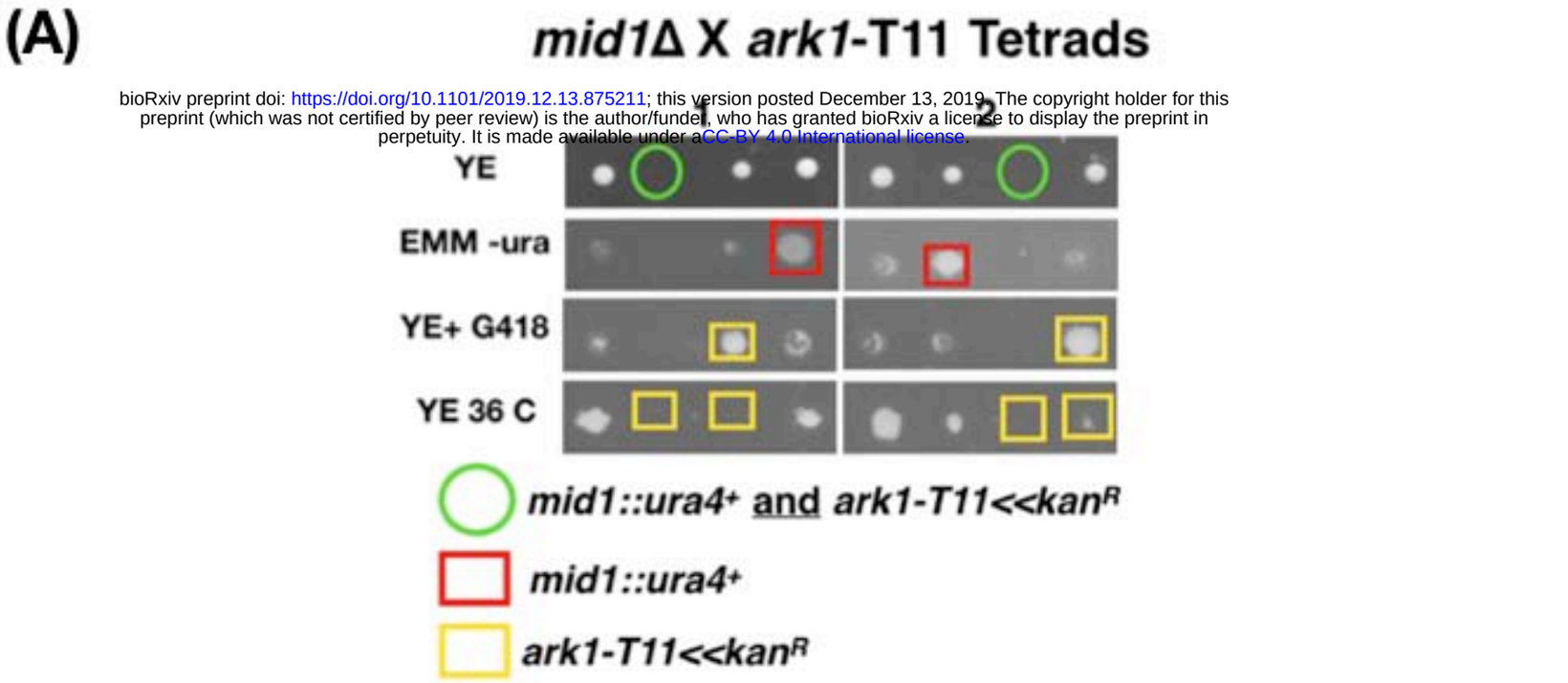

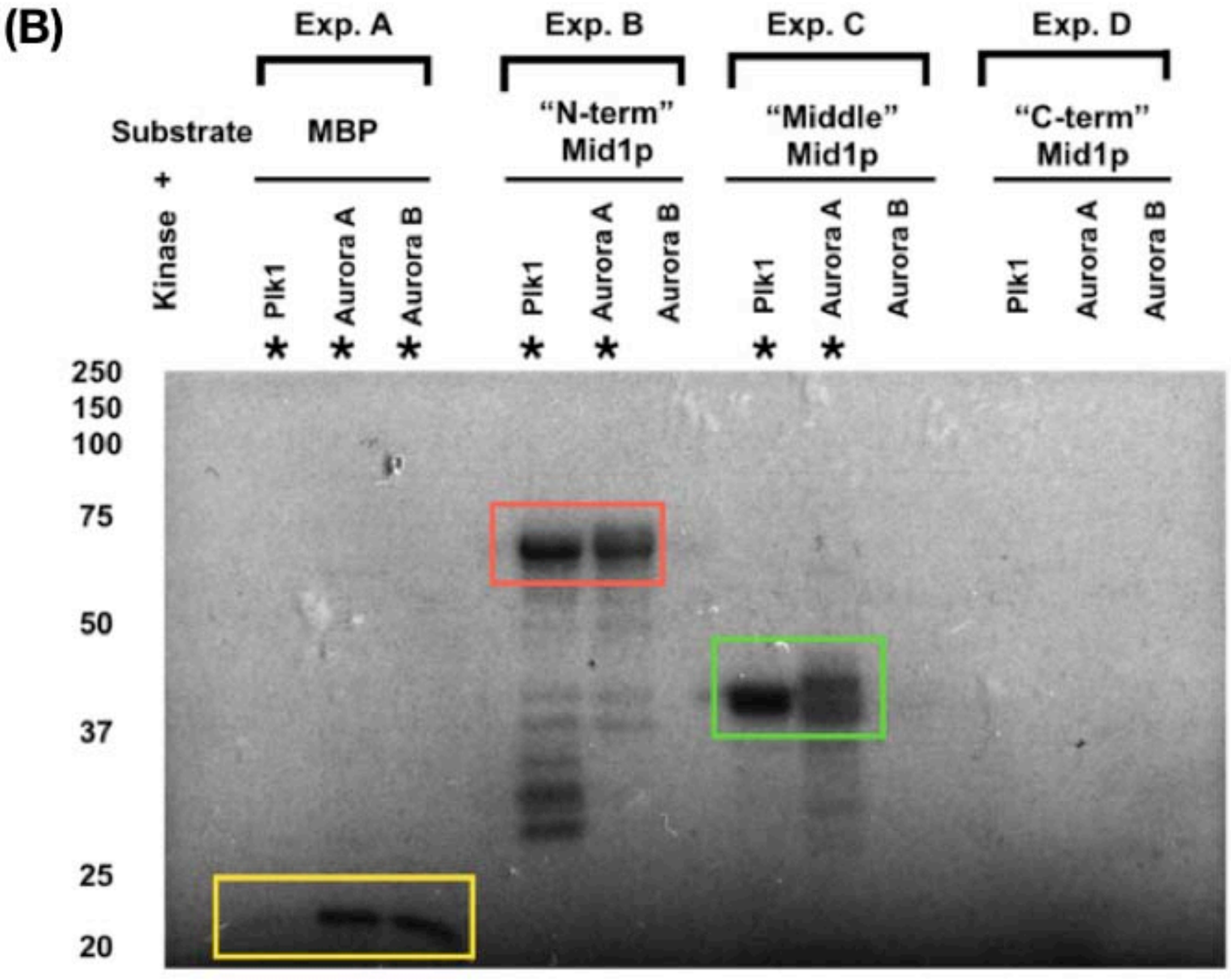

perpetuity. It is made available under aCC-BY 4.0 International license.

(A)

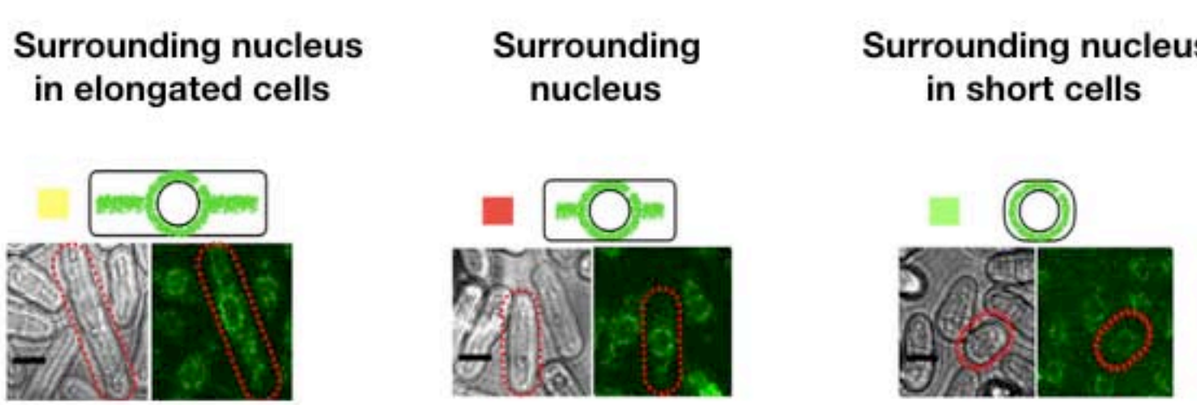

(B)

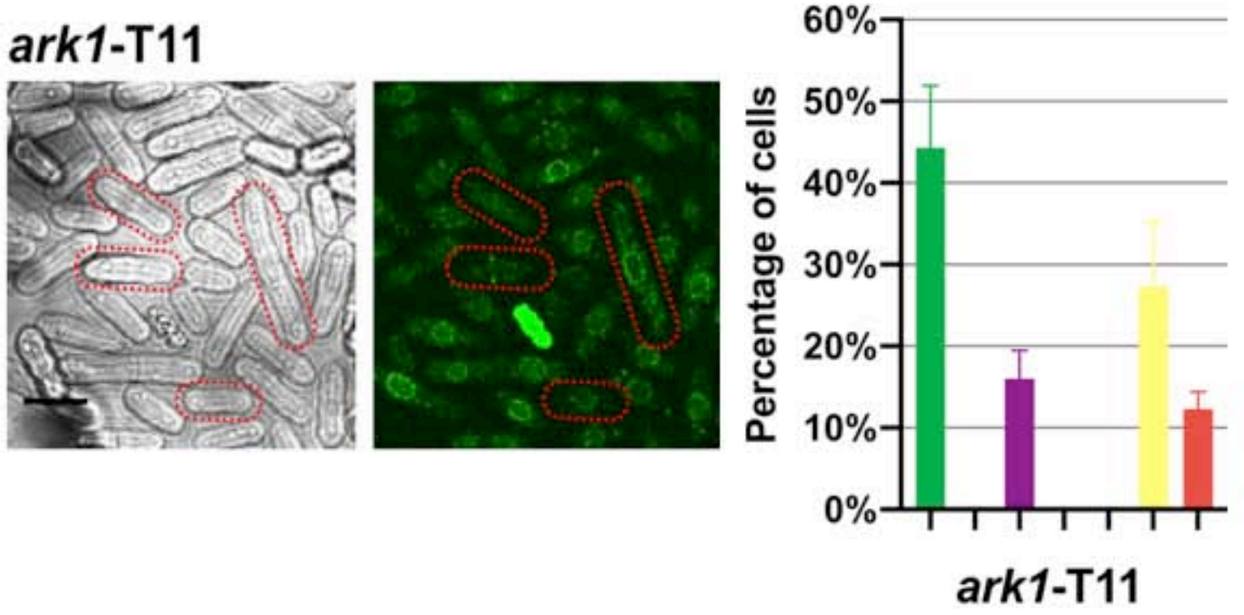

(C)

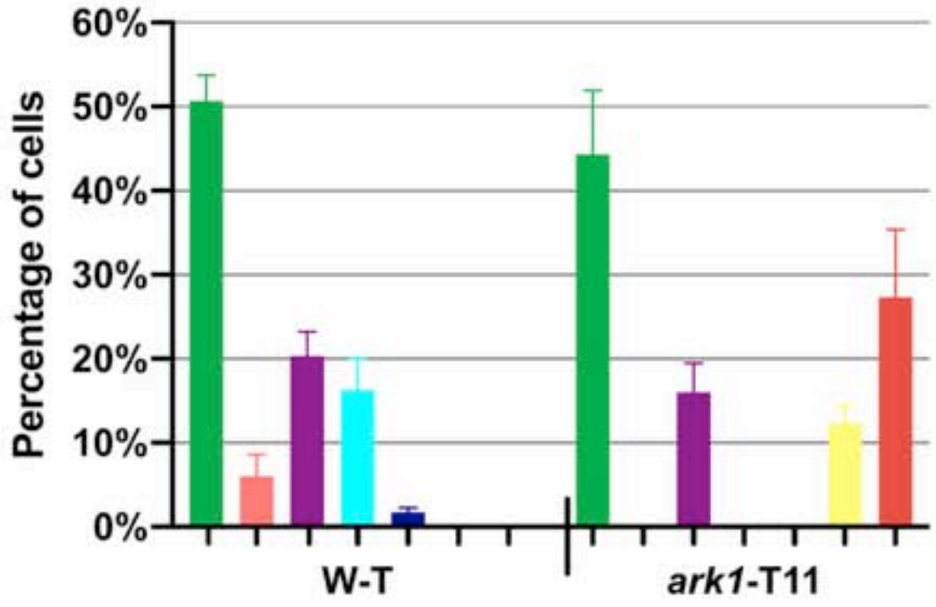

(D)

(E)

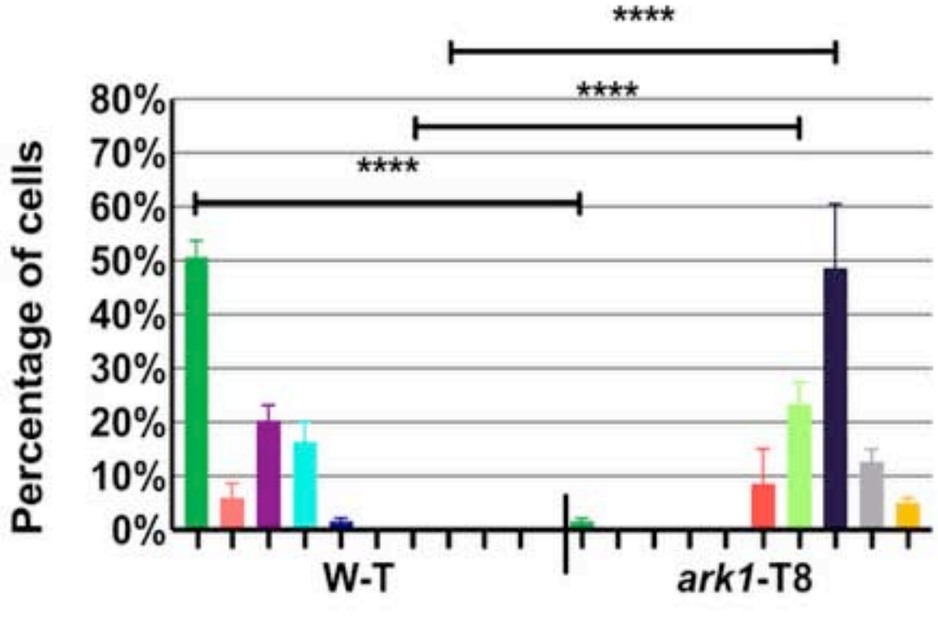

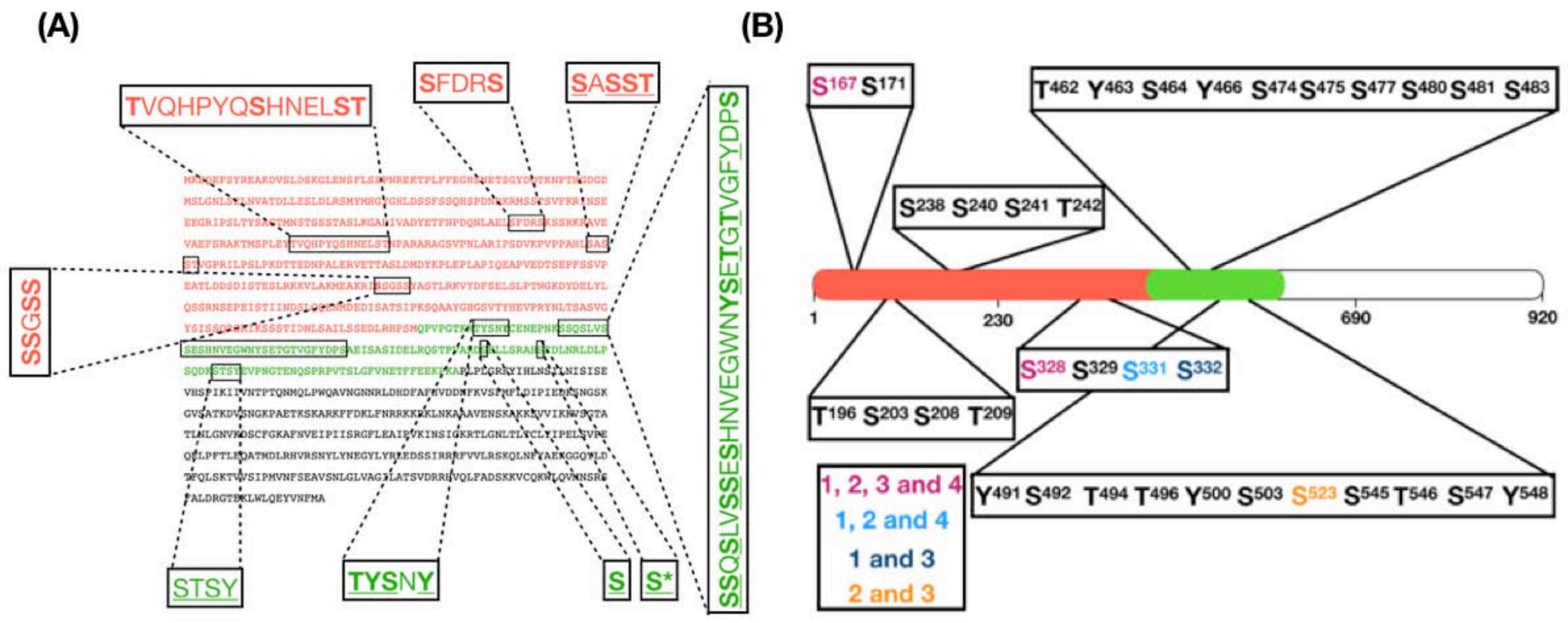
(A)
TVQHPYQSHNELST
SFDRS
SASST
SSGSS
STSY
TYSNY
S
S*
SSQSLVSSESHNVEGWNYSETGTVGFYDPS
(B)
S167 S171
T462 Y463 S464 Y466 S474 S475 S477 S480 S481 S483
S238 S240 S241 T242
1
230
690
920
S328 S329 S331 S332
T196 S203 S208 T209
Y491 S492 T494 T496 Y500 S503 S523 S545 T546 S547 Y548
1, 2, 3 and 4
1, 2 and 4
1 and 3
2 and 3

(A)

Experiment A
aurora A

Experiment B
plk1

MBP N-term S167A S328A S331A S332A Multiple

MBP N-term S167A S328A S331A S332A Multiple

kDa
250
150
100
75
50
37
25
20
15

* **

SDS-PAGE

Autoradiograph

(B)

Experiment A
aurora A

Experiment B
plk1

MBP Middle S523A S531A Multiple

MBP Middle S523A S531A Multiple

kDa
250
150
100
75
50
37
25
20
15

* **

Plk1

SDS-PAGE

Plk1

Autoradiograph

bioRxiv preprint doi: https://doi.org/10.1101/2019.12.13.875211; this version posted December 13, 2019. The copyright holder for this preprint (which was not certified by peer review) is the author/funder, who has granted bioRxiv a license to display the preprint in perpetuity. It is made available under aCC-BY 4.0 International license.

(A)

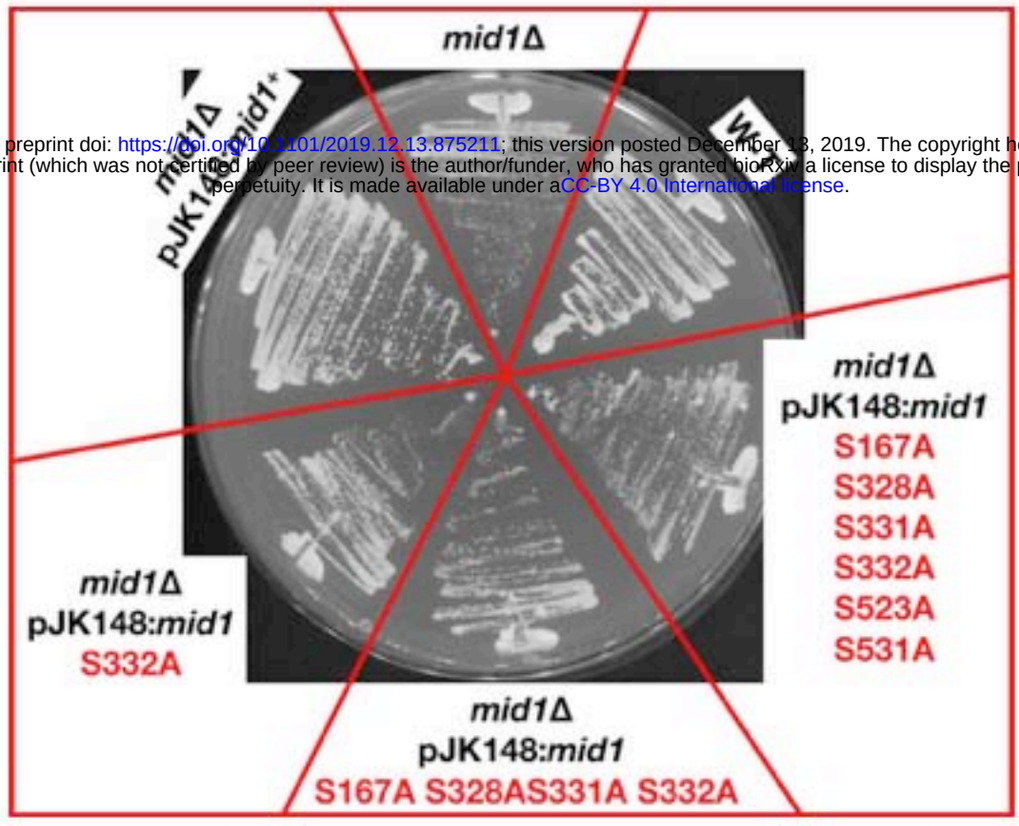

(B)

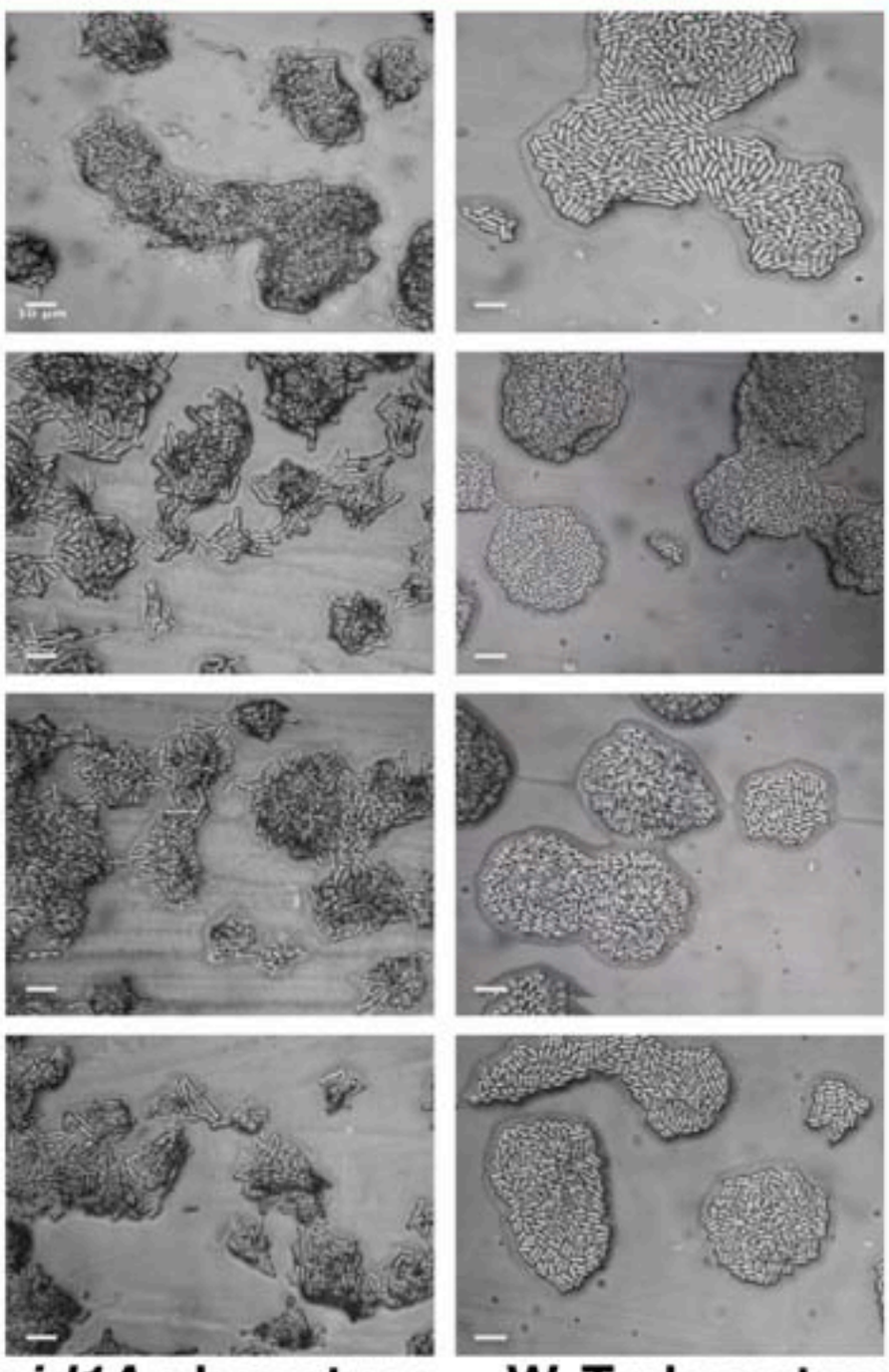

bioRxiv preprint doi: https://doi.org/10.1101/2019.12.13.875211; this version posted December 13, 2019. The copyright holder for this preprint (which was not certified by peer review) is the author/funder, who has granted bioRxiv a license to display the preprint in perpetuity. It is made available under aCC-BY 4.0 International license.

W-T

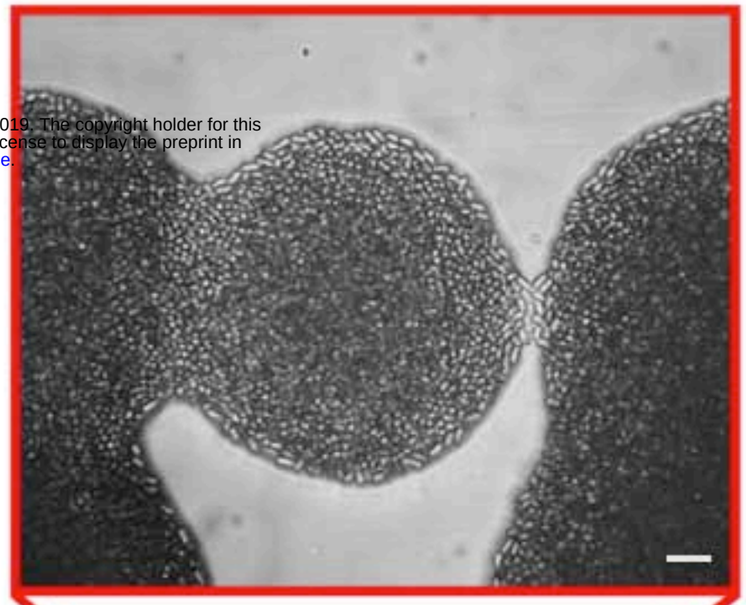

mid1Δ
pJK148:*mid1*S523D S531D

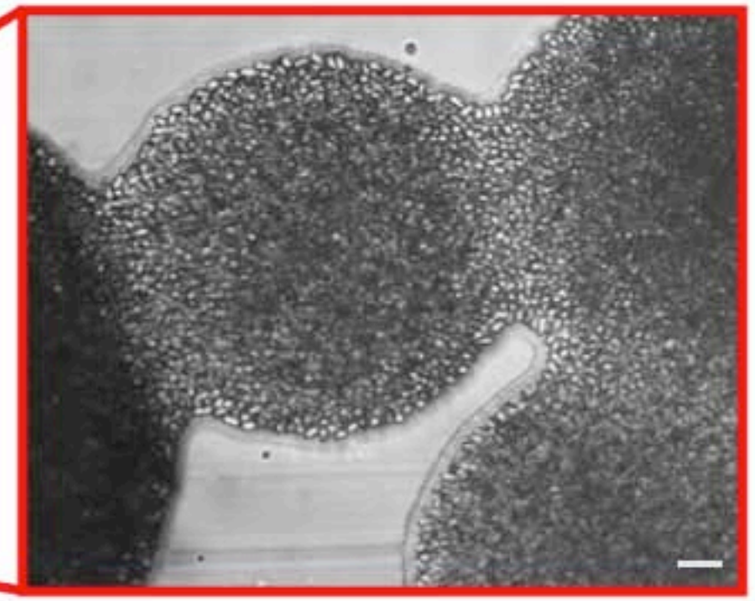

vps4Δ

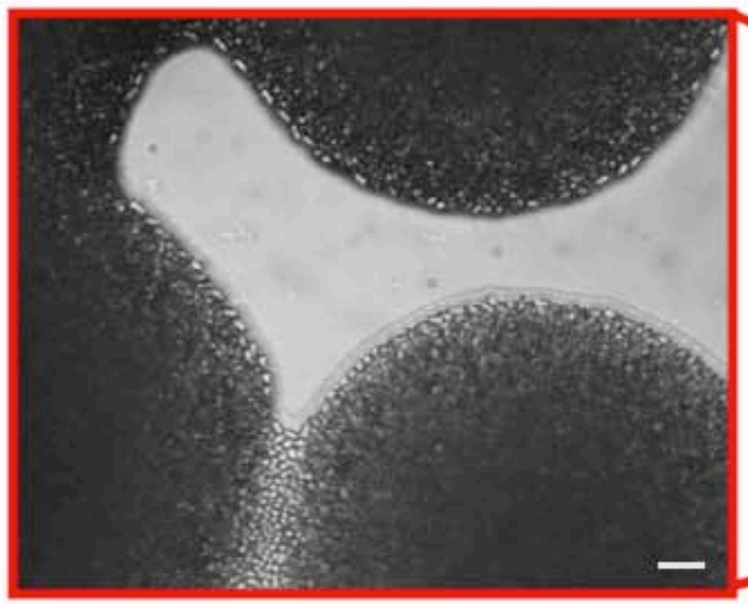

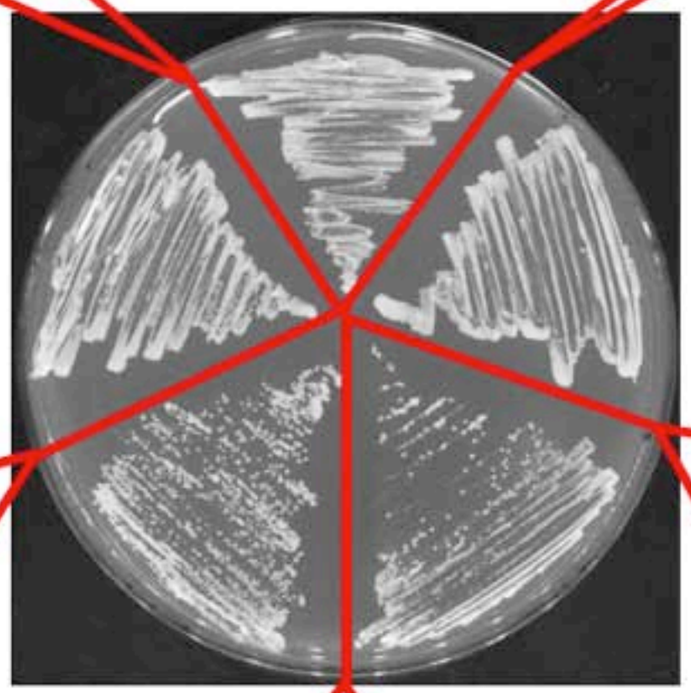

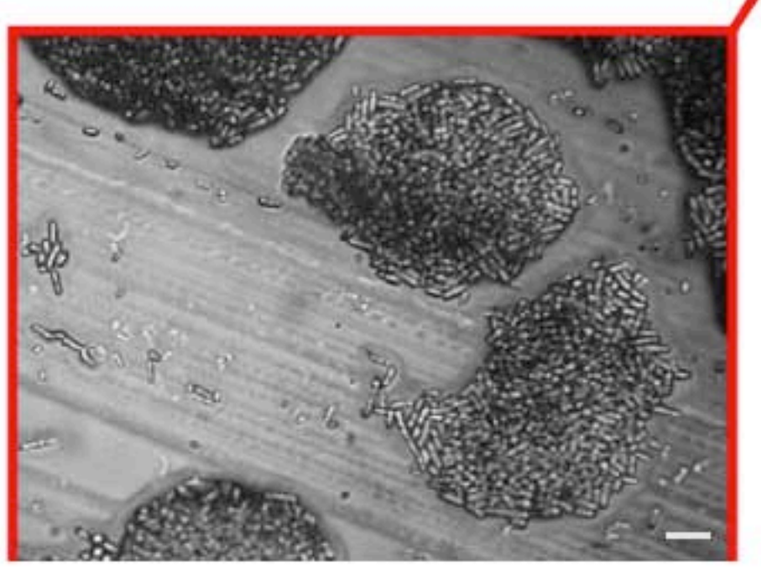

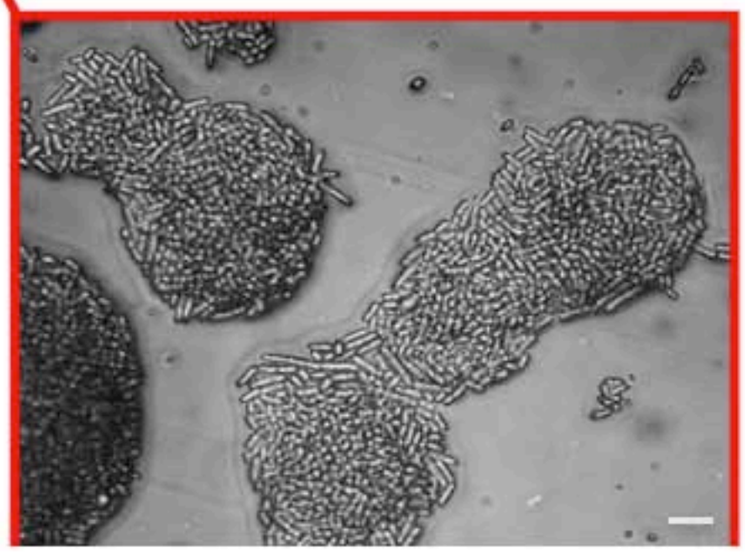

mid1Δ
pJK148:*mid1*S523D S531D *vps4Δ*

mid1Δ
pJK148:*mid1*S523D S531D *vps4Δ*

bioRxiv preprint doi: https://doi.org/10.1101/2019.12.13.875211; this version posted December 13, 2019. The copyright holder for this preprint (which was not certified by peer review) is the author/funder, who has granted bioRxiv a licence to display the preprint in perpetuity. It is made available under aCC-BY 4.0 International license.

A

Early interphase

Late interphase

Metaphase

Anaphase

Septation

Mid1p

Nucleus

CR

Septum

B

C-terminal Mid1p

N-terminal Mid1p

P

Plo1p

Incorporation of Mid1p into Nodes

Rng2p

Gef2p

Cdr2p

C

Plasma Membrane

C-terminal Mid1p

Vps4p

N-terminal Mid1p

Gef2p

Rng2p

Cdr2p

L3

712

654

C2

Connector

C

N

PH

bioRxiv preprint doi: https://doi.org/10.1101/2019.12.13.875211; this version posted December 13, 2019. The copyright holder for this preprint (which was not certified by peer review) is the author/funder, who has granted bioRxiv a license to display the preprint in perpetuity. It is made available under aCC-BY 4.0 International license.

S1 Table. *S. pombe* strains used in this study. "GG" number refers to the laboratory reference collection. All strains *ade*$^-$, unless indicated.

GG No.	Genotype	Annotation
1	h$^-$ 972	wild-type (W-T)
397	h$^+$ *ade6-210 leu1-32 ura4-D18*	
400	h$^-$ *ade6-216 leu1-32 ura4-D18*	
1129	h$^-$ *mid1*::*ura4*$^+$ *ura4-D18 leu1-32*	*mid1*Δ
1347	pmid-*mid1*-4GFP (integrated; pAP221; *leu1*$^+$) h$^-$ *dmf1*::*ura4*$^+$ *ura4*-D18 *leu1-32*	Mid1p-GFP
1349	pmid-NLS*-*mid1*-GFP (integrated; pAP167#2; *leu1*$^+$) h$^-$ *dmf1*::*ura4*$^+$ *ura4-D18 leu1-32*	
1384	pAM19 (D450-506 *mid1*:*12myc*:*leu1*$^+$) h$^-$ *dmf1*::*ura4*$^+$*ura4-D18 leu1-32*	
1388	pAM23 (*NLS*mid1*:*12myc*:*leu1*$^+$) h$^-$ *dmf1*::*ura4*$^+$ *ura4-D18 leu1-32*	
1554	h$^+$ *dmf1*::*kanMX4 ura4-D18 leu1-32 ade*$^+$	*mid1*Δ
1622	h$^-$ *vps4*::*ura4*$^+$ *leu1-32 ura4-D18 ade*$^+$	*vps4*Δ
2417	h$^+$ *ark1*-T11<<kanR *leu1-32 ade*$^+$	*ark1*-T11
2432	h$^+$ *ark1*-T8<<kanR *leu1-32 ade*$^+$	*ark1*-T8
2673	h$^+$ *vps4*::*ura4*$^+$ *leu1-32 ura4-D18 ade*$^+$	*vps4*Δ
2674	pmid-*mid1*-4GFP (integrated; pAP221; *leu1*$^+$) h$^-$ *dmf1*::*ura4*$^+$*ura4-D18? leu1-32 vps4*::*ura4*$^+$	*vps4*Δ Mid1p-GFP
2709	pmid-*mid1*-4GFP (integrated; pAP221; *leu1*$^+$) h$^-$ *dmf1*::*ura4*$^+$*ura4-D18? leu1-32 vps4*::*ura4*$^+$	*vps4*Δ Mid1p-GFP
2886	pmid-*mid1*-4GFP (integrated; pAP221; *leu1*$^+$) h$^-$ *dmf1*::*ura4*$^+$*ura4-D18? leu1-32 ark1*-T11<<kanR	*ark1-T11* Mid1p-GFP
2922	pmid-mid1-4GFP (integrated; pAP221; *leu1*$^+$) h$^+$ *dmf1*::*ura4*$^+$ *ura4-D18 leu1-32 ark1*-T8<<kanR	*ark1-T8* Mid1p-GFP
3100	NLS* *mid1*:*12myc*:*leu1*$^+$ h$^-$ *dmf1*::*ura4*$^+$ *vps4*::*ura4*$^+$ *ura4-D18 leu1-32*	
3107	D450-506 *mid1*:*12myc*:*leu1*$^+$ h$^-$ *dmf1*::*ura4*$^+$ *vps4*::*ura4*$^+$ *ura4-D18 leu1-32*	
3181	pJK148:*mid1*$^+$ (wild-type) h$^-$ *mid1*::*ura4*$^+$ *ura4-D18 leu1-32*	*mid1*Δ pJK148:*mid1*$^+$
3185	pJK148:*mid1* S523 to A523 h$^-$ *mid1*::*ura4*$^+$ *ura4-D18 leu1-32*	
3189	pJK148:*mid1* S523 to D523 h$^-$ *mid1*::*ura4*$^+$ *ura4-D18 leu1-32*	
3193	pJK148:*mid1* S531 to A531 h$^-$ *mid1*::*ura4*$^+$ *ura4-D18 leu1-32*	
3197	pJK148:*mid1* S531 to D531 h$^-$ *mid1*::*ura4*$^+$ *ura4-D18 leu1-32*	
3201	pJK148:*mid1* S523+S531 to A523+A531 h$^-$ *mid1*::*ura4*$^+$ *ura4-D18 leu1-32*	
3205	pJK148:*mid1* S523+S531 to D523+D531 h$^-$ *mid1*::*ura4*$^+$ *ura4-D18 leu1-32*	
3218	pJK148:*mid1* S523 to A523 h$^?$ *mid1*::*ura4*$^+$ *ark1*-T11<<kanR *ade*$^+$	
3224	pJK148:*mid1* S523 to A523 h$^?$ *mid1*::*ura4*$^+$ *vps4*::*ura4+ura4-D18 leu1-32*	
3230	pJK148:*mid1* S523 to D523 h$^?$ *mid1*::*ura4*$^+$ *ark1*-T11<<kanR *ura4-C190T leu1-32*	

bioRxiv preprint doi: https://doi.org/10.1101/2019.12.13.875211; this version posted December 13, 2019. The copyright holder for this preprint (which was not certified by peer review) is the author/funder, who has granted bioRxiv a license to display the preprint in perpetuity. It is made available under aCC-BY 4.0 International license.

3235	pJK148:*mid1* S531 to A531 h$^{?}$ *mid1*::*ura4*$^{+}$ *ark1*-T11<<kanR *ura4-C190T leu1-32*
3239	pJK148:*mid1* S531 to D531 h$^{?}$ *mid1*::*ura4*$^{+}$ *ark1*-T11<<kanR *ura4-C190T leu1-32*
3242	pJK148:*mid1* S523 to A523+S531 to A531 h$^{?}$ *mid1*::*ura4*$^{+}$ *ark1*-T11<<kanR *ura4-C190T leu1-32*
3246	pJK148:*mid1* S523+S531 to D523+D531 h$^{?}$ *mid1*::*ura4*$^{+}$ *ark1*-T11<<kanR *ura4-C190T leu1-32*
3250	pJK148:*mid1* (wild-type) *mid1*Δ pJK148:*mid1*$^{+}$ *ark1*-T11 h$^{?}$ *mid1*::*ura4*$^{+}$ *ark1*-T11<<kanR *ura4-C190T leu1-32*
3257	pJK148:*mid1* S523+S531 to D523+D531 h^{-} *mid1*::*ura4*$^{+}$ *vps4*::*ura4+ ura4-D18 leu1-32*
3258	pJK148:*mid1* S523+S531 to D523+D531 h^{-} *mid1*::*ura4*$^{+}$ *vps4*::*ura4+ ura4-D18 leu1-32*
3260	pJK148:*mid1* S523+S531 to A523+A531 h$^{?}$ *mid1*::*ura4*$^{+}$ *vps4*::*ura4*$^{+}$ *ura4-D18 leu1-32*
3264	pJK148:mid1 S531 to D531 h$^{?}$ *mid1*::*ura4*$^{+}$ *vps4*::*ura4*$^{+}$ *ura4-D18 leu1-32*
3267	pJK148:*mid1* S167 to A167 h^{-} *mid1*::*ura4*$^{+}$ *ura4-D18 leu1-32*
3271	pJK148:*mid1* S167 to D167 h^{-} *mid1*::*ura4*$^{+}$ *ura4-D18 leu1-32*
3275	pJK148:*mid1* S328 to A328 h^{-} *mid1*::*ura4*$^{+}$ *ura4-D18 leu1-32*
3280	pJK148:*mid1* S328 to D328 h^{-} *mid1*::*ura4*$^{+}$ *ura4-D18 leu1-32*
3283	pJK148:*mid1* S331 to A331 h^{-} *mid1*::*ura4*$^{+}$ *ura4-D18 leu1-32*
3290	pJK148:*mid1* S331 to D331 h^{-} *mid1*::*ura4*$^{+}$ *ura4-D18 leu1-32*
3291	pJK148:*mid1* S332 to A332 h^{-} *mid1*::*ura4*$^{+}$ *ura4-D18 leu1-32*
3295	pJK148:*mid1* S332 to D332 h^{-} *mid1*::*ura4*$^{+}$ *ura4-D18 leu1-32*
3299	pJK148:*mid1* S167+S328+S331+S332 to A167+A328+A331+A332 h^{-} *mid1*::*ura4*$^{+}$ *ura4-D18 leu1-32*
3305	pJK148:*mid1* S167+S328+S331+S332 to D167+D328+D331+D332 h^{-} *mid1*::*ura4*$^{+}$ *ura4-D18 leu1-32*
3307	pJK148:*mid1* S167+S328+S331+S332+S523+S531 to A167+A328+A331+A332+A523+A531 h^{-} *mid1*::*ura4*$^{+}$ *ura4-D18 leu1-32*
3311	pJK148:*mid1* S167+S328+S331+S332+S523+S531 to D167+D328+D331+D332+D523+D531 h^{-} *mid1*::*ura4*$^{+}$ *ura4-D18 leu1-32*
3315	pJK148:*mid1* S523 to D523 h$^{?}$ *mid1*::*ura4*$^{+}$ *vps4*::*ura4+ ura4-D18 leu1-32*
3318	pJK148:*mid1* S531 to A531 h$^{?}$ *mid1*::*ura4*$^{+}$ *vps4*::*ura4+ ura4-D18 leu1-32*
3321	pJK148:*mid1* S167 to A167 h$^{?}$ *mid1*::*ura4*$^{+}$ *ark1*-T11<<kanR ura4-C190T *leu1-32*
3324	JK148:*mid1* S167 to D167 h$^{?}$ *mid1*::*ura4*$^{+}$ *ark1*-T11<<kanR *ura4-C190T leu1-32*
3327	pJK148:*mid1* S328 to A328 h$^{?}$ *mid1*::*ura4*$^{+}$ *ark1*-T11<<kanR *ura4-C190T leu1-32*
3330	pJK148:*mid1* S328 to D328 h$^{?}$ *mid1*::*ura4*$^{+}$ *ark1*-T11<<kanR *ura4*-C190T *leu1-32*
3333	pJK148:*mid1* S331 to A331 h$^{?}$ *mid1*::*ura4*$^{+}$ *ark1*-T11<<kanR *ura4-C190T leu1-32*

bioRxiv preprint doi: https://doi.org/10.1101/2019.12.13.875211; this version posted December 13, 2019. The copyright holder for this preprint (which was not certified by peer review) is the author/funder, who has granted bioRxiv a license to display the preprint in perpetuity. It is made available under aCC-BY 4.0 International license.

3336	pJK148:*mid1* S331 to D331 h$^{?}$ *mid1*::*ura4*$^{+}$ *ark1*-T11<<kanR *ura4-C190T leu1-32*
3339	pJK148:*mid1* S332 to A332 h$^{?}$ *mid1*::*ura4*$^{+}$ *ark1*-T11<<kanR *ura4-C190T leu1-32*
3342	pJK148:*mid1* S332 to D332 h$^{?}$ *mid1*::*ura4*$^{+}$ *ark1*-T11<<kanR *ura4-C190T leu1-32*
3345	pJK148:*mid1* S167+S328+S331+S332 to A167+A328+A331+A332 h$^{?}$ *mid1*::*ura4*$^{+}$ *ark1*-T11<<kanR *ura4-C190T leu1-32*
3349	pJK148:*mid1* S167+S328+S331+S332 to D167+D328+D331+D332 h$^{?}$ *mid1*::*ura4*$^{+}$ *ark1*-T11<<kanR *ura4-C190T leu1-32*
3352	pJK148:*mid1* S167+S328+S331+S332+S523+S531 to A167+A328+A331+A332+A523+A531 h$^{?}$ *mid1*::*ura4*$^{+}$ *ark1*-T11<<kanR *ura4-C190T leu1-32*
3355	pJK148:*mid1* S167+S328+S331+S332+S523+S531 to D167+D328+D331+D332+D523+D531 h$^{?}$ *mid1*::*ura4*$^{+}$ *ark1*-T11<<kanR *ura4-C190T leu1-32*
3375	pJK148:*mid1* S167 to A167 h$^{?}$ *mid1*::*ura4*$^{+}$ *plo1-ts35 ura4-D18 leu1-32*
3377	pJK148:mid1 S167 to D167 h$^{?}$ *mid1*::*ura4*$^{+}$ *plo1-ts35 ura4-D18 leu1-32*
3383	pJK148:*mid1* S167 to A167 h$^{?}$ *mid1*::*ura4*$^{+}$ *vps4*::*ura4*$^{+}$ *ura4-D18 leu1-32*
3392	pJK148:*mid1* S328 to A328 h$^{?}$ *mid1*::*ura4*$^{+}$ *plo1-ts35 ura4-D18 leu1-32*
3386	pJK148:*mid1* S328 to D328 h$^{?}$ *mid1*::*ura4*$^{+}$ *plo1-ts35 ura4-D18 leu1-32*
3392	pJK148:*mid1* S328 to A328 h$^{?}$ *mid1*::*ura4*$^{+}$ *plo1-ts35 ura4-D18 leu1-32*
3397	pJK148:*mid1* S331 to A331 h$^{?}$ *mid1*::*ura4*$^{+}$ *plo1-ts35 ura4-D18 leu1-32*
3400	pJK148:*mid1* S332 to A332 h$^{?}$ *mid1*::*ura4*$^{+}$ *plo1-ts35 ura4-D18 leu1-32*
3403	pJK148:*mid1* S523 to D523 h^{-} *mid1*::*ura4*$^{+}$ *plo1-ts35 ura4-D18 leu1-32*
3407	pJK148:*mid1* S523 to A523 h^{-} *mid1*::*ura4*$^{+}$ *plo1-ts35 ura4-D18 leu1-32*
3411	pJK148:*mid1* S332 to D332 h^{-} *mid1*::*ura4*$^{+}$ *plo1-ts35 ura4-D18 leu1-32*
3415	pJK148:*mid1* S531 to A531 h^{-} *mid1*::*ura4*$^{+}$ *plo1-ts35 ura4-D18 leu1-32*
3419	pJK148:*mid1* S167+S328+S331+S332 to A167+A328+A331+A332 h^{-} *mid1*::*ura4*$^{+}$ *plo1-ts35 ura4-D18 leu1-32*
3422	pJK148:*mid1* S167+S328+S331+S332 to D167+D328+D331+D332 h^{-} *mid1*::*ura4*$^{+}$ *plo1-ts35 ura4-D18 leu1-32*
3425	pJK148:*mid1* S167+S328+S331+S332+S523+S531 to A167+A328+A331+A332+A523+A531 h^{-} *mid1*::*ura4*$^{+}$ *plo1-ts35 ura4-D18 leu1-32*
3428	pJK148:*mid1* S531 to D531 h^{-} *mid1*::*ura4*$^{+}$ *plo1-ts35 ura4-D18 leu1-32*
3437	pJK148:*mid1*$^{+}$ (wild-type) *mid1*Δ pJK148:*mid1*$^{+}$ *plo1-ts35* h^{-} *mid1*::*ura4*$^{+}$ *plo1-ts35 ura4-D18 leu1-32*
3441	pJK148:*mid1* S167+S328+S331+S332+S523+S531 to D167+D328+D331+D332+D523+D531 h- *mid1*::*ura4*$^{+}$ *plo1-ts35 ura4-D18 leu1-32*
3444	pJK148:*mid1* S523 to A523 + S531 to A531 h^{-} *mid1*::*ura4*$^{+}$ *plo1-ts35 ura4-D18 leu1-32*
3447	pJK148:*mid1* S523 to D523 + S531 to D531 h- *mid1*::*ura4*+ *plo1-ts35 ura4-D18 leu1-32*

bioRxiv preprint doi: https://doi.org/10.1101/2019.12.13.875211; this version posted December 13, 2019. The copyright holder for this preprint (which was not certified by peer review) is the author/funder, who has granted bioRxiv a license to display the preprint in perpetuity. It is made available under aCC-BY 4.0 International license.

3450	pJK148:*mid1* S167 to A167 h$^{?}$ *mid1*::*ura4*$^{+}$ *vps4*::*ura4+ ura4-D18 leu1-32*
3456	pJK148:*mid1* S328 to A328 h$^{?}$ *mid1*::*ura4*$^{+}$ *vps4*::*ura4+ ura4-D18 leu1-32*
3461	pJK148:*mid1* S167+S328+S331+S332 to D167+D328+D331+D332 h$^{?}$ *mid1*::*ura4*$^{+}$ *vps4*::*ura4+ ura4-D18 leu1-32*
3463	pJK148:*mid1* S167+S328+S331+S332+S523+S531 to D167+D328+D331+D332+D523+D531 h$^{?}$ *mid1*::*ura4*$^{+}$ *vps4*::*ura4+ ura4-D18 leu1-32*
3467	pJK148:*mid1* S167+S328+S331+S332+S523+S531 to A167+A328+A331+A332+A523+A531 h$^{?}$ *mid1*::*ura4*$^{+}$ *vps4*::*ura4+ ura4-D18 leu1-32*
3469	pJK148:*mid1* S332 to D332 h$^{?}$ *mid1*::*ura4*$^{+}$ *vps4*::*ura4+ ura4-D18 leu1-32*
3473	pJK148:*mid1* S332 to A332 h$^{?}$ *mid1*::*ura4*$^{+}$ *vps4*::*ura4+ ura4-D18 leu1-32*
3481	pJK148:*mid1* S328 to D328 h$^{?}$ *mid1*::*ura4*$^{+}$ *vps4*::*ura4+ ura4-D18 leu1-32*
3485	pJK148:*mid1* S331 to A331 h$^{?}$ *mid1*::*ura4*$^{+}$ *vps4*::*ura4+ ura4-D18 leu1-32*
3486	pJK148:*mid1*$^{+}$ (wild-type) *mid1*Δ pJK148:*mid1*$^{+}$ *vps4*Δ h$^{?}$ *mid1*::*ura4*$^{+}$ *vps4*::*ura4+ ura4-D18 leu1-32*
3488	pJK148:*mid1*$^{+}$ S167+S328+S331+S332 to A167+A328+A331+A332 h$^{?}$ *mid1*::*ura4*$^{+}$ *vps4*::*ura4+ ura4-D18 leu1-32*

3

4

bioRxiv preprint doi: https://doi.org/10.1101/2019.12.13.875211; this version posted December 13, 2019. The copyright holder for this preprint (which was not certified by peer review) is the author/funder, who has granted bioRxiv a license to display the preprint in perpetuity. It is made available under aCC-BY 4.0 International license.

S2 Table. Vector DNA constructs used in this study. "GB" number refers to the laboratory reference collection.

GB No.	Abbreviated plasmid vector description
880	pET-14b - His tagged, Vps4p full length, *Nde* I/*Bam* HI Invitrogen order 13AB6ZFP
881	pGEX4T1 - GST tagged, Mid1p 1-453, *Bam* HI/*Xho* I - "N-term" GenScript order U2640BJ110
882	pGEX4T1 - GST tagged, Mid1p 452-579, *Bam* HI/*Xho* I - "Middle"
883	pGEX4T1 - GST tagged, Mid1p 578-799, *Bam* HI/*Xho* I
884	pGEX4T1 - GST tagged, Mid1p 798-920, *Bam* HI/*Xho* I - "C-term"
889	pET-14b - His tagged, Myo2p C-terminus amino acids 1394-1526, *Nde* I/*Bam* HI GenScript order U9540CD270_2
907	*mid1*$^{+}$ wild-type + 1 kb upstream of ORF - 3,853 base pairs in total *Kpn* I/*Sac* I fragment cloned into pJK148 GenScript order U2002DH100
909	*mid1* mutant (1) S523 to A523 in pJK148
911	*mid1* mutant (1) S523 to D523 in pJK148
913	*mid1* mutant (1) S531 to A531 in pJK148
915	*mid1* mutant (1) S531 to D531 in pJK148
917	*mid1* mutant (2) S523 to A523 + S531 to A531 in pJK148
919	*mid1* mutant (2) S523 to D523 + S531 to D531 in pJK148
923	*mid1* mutant (1) S167 to A167 in pJK148 GenScript order U894VEB050
924	*mid1* mutant (1) S167 to D167 in pJK148
925	*mid1* mutant (1) S328 to A328 in pJK148
926	*mid1* mutant (1) S328 to D328 in pJK148
927	*mid1* mutant (1) S331 to A331 in pJK148
928	*mid1* mutant (1) S331 to D331 in pJK148
929	*mid1* mutant (1) S332 to A332 in pJK148
930	*mid1* mutant (1) S332 to D332 in pJK148
931	*mid1* mutant (4) S167 to A167 + S328 to A328 + S331 to A331+ S332 to A332 in pJK148
932	*mid1* mutant (4) S167 to D167 + S328 to D328 + S331 to D331+ S332 to D332 in pJK148
933	*mid1* mutant (6) S167 to A167 + S328 to A328 + S331 to A331+ S332 to A332 + S523 to A523 + S531 to A531 in pJK148
934	*mid1* mutant (6) S167 to D167 + S328 to D328 + S331 to D331+ S332 to D332 + S523 to D523 + S531 to D531 in pJK148
935	pGEX4T1 - GST tagged, Mid1p 1-453, *Bam* HI/*Xho* I - "N-term" S167 to A167 GenScript order U8198EF120
936	pGEX4T1 - GST tagged, Mid1p 1-453, *Bam* HI/*Xho* I - "N-term" S328 to A328
937	pGEX4T1 - GST tagged, Mid1p 1-453, *Bam* HI/*Xho* I - "N-term" S331 to A331
938	pGEX4T1 - GST tagged, Mid1p 1-453, *Bam* HI/*Xho* I - "N-term" S332 to A332
939	pGEX4T1 - GST tagged, Mid1p 1-453, *Bam* HI/*Xho* I - "N-term" S167 to A167 + S328 to A328 + S331 to A331 + S332 to A332
940	pGEX4T1 - GST tagged, Mid1p 452-579, *Bam* HI/*Xho* I - "Middle" S523 to A523
941	pGEX4T1 - GST tagged, Mid1p 452-579, *Bam* HI/*Xho* I - "Middle" S531 to A531
942	pGEX4T1 - GST tagged, Mid1p 452-579, *Bam* HI/*Xho* I - "Middle" S523 to A523 + S531 to A531

bioRxiv preprint doi: https://doi.org/10.1101/2019.12.13.875211; this version posted December 13, 2019. The copyright holder for this preprint (which was not certified by peer review) is the author/funder, who has granted bioRxiv a license to display the preprint in perpetuity. It is made available under aCC-BY 4.0 International license.

S3 Table. Summary of *S. pombe* global proteomic studies of identified Mid1p phospho-sites.

Study	Total number of phosphory-lation events	Mid1p phospho-sites				Reference
		Ref. No.	**Mid1p Residue position**	Ref. No.	**Mid1p Residue position**	
1	8000	7140	**S15**	7150	**S335**	[21]
		7141	**S18**	7151	**S110**	
		7142	**S167**	7152	**S112**	
		7144	**S24**	7153	**S344**	
		7145	**S27**	7154	**S347**	
		7146	**S328**	9637	**T336**	
		7148	**S331**	9638	**T111**	
		7149	**S332**	10,040	**Y333**	
2	3682	3150	**S7**	3156	**S328**	[22]
		3151	**S167**	3157	**S331**	
		3153	**S24**	3158	**S109**	
		3154	**S27**	3159	**S344**	
		3155	**28**	3160	**S347**	
				20,982	**S523**	
3	12,524	10,736	**S218**	10,749	**S434**	[23]
		10,738	**S24**	10,750	**T435**	
		5831	**S167**	10,755	**S440**	
		10,742	**S331**	10,756	**S444**	
		10,743	**S328**	10,757	**S445**	
		10,744	**S332**	10,758	**S532**	
		10,745	**T336**	10,759	**S527**	
		10,746	**S403**	10,760	**S531**	
		10,747	**S432**	10,764	**T34**	
		10,748	**S433**	10,765	**S42**	
				10,767	**S335**	
4	7298	5835	**S167**	5844	**S403**	[24]
		5836	**S218**	5845	**S434**	
		5837	**S24**	5846	**S444**	
		5838	**S27**	5847	**S531**	
		5839	**S28**	5848	**S541**	
		5840	**S328**	5849	**S7**	
		5842	**S331**	5850	**T34**	
		5843	**S395**	5851	**T405**	

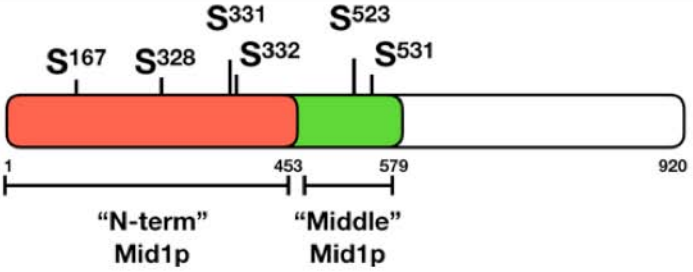

Amino acid	167	328	331	332	523	531	GG No.
mid1 W-T	S	S	S	S	S	S	3181
S167A	A	-	-	-	-	-	3267
S167D	D	-	-	-	-	-	3271
S328A	-	A	-	-	-	-	3275
S328D	-	D	-	-	-	-	3279
S331A	-	-	A	-	-	-	3283
S331D	-	-	D	-	-	-	3287
S332A	-	-	-	A	-	-	3291
S332D	-	-	-	D	-	-	3295
S523A	-	-	-	-	A	-	3185
S523D	-	-	-	-	D	-	3189
S531A	-	-	-	-	-	A	3193
S531D	-	-	-	-	-	D	3197
Multi	A	A	A	A	-	-	3299
Multi	D	D	D	D	-	-	3303
Multi	-	-	-	-	A	A	3201
Multi	-	-	-	-	D	D	3205
Multi	A	A	A	A	A	A	3307
Multi	D	D	D	D	D	D	3311

bioRxiv preprint doi: https://doi.org/10.1101/2019.12.13.875211; this version posted December 13, 2019. The copyright holder for this preprint (which was not certified by peer review) is the author/funder, who has granted bioRxiv a license to display the preprint in perpetuity. It is made available under aCC-BY 4.0 International license.

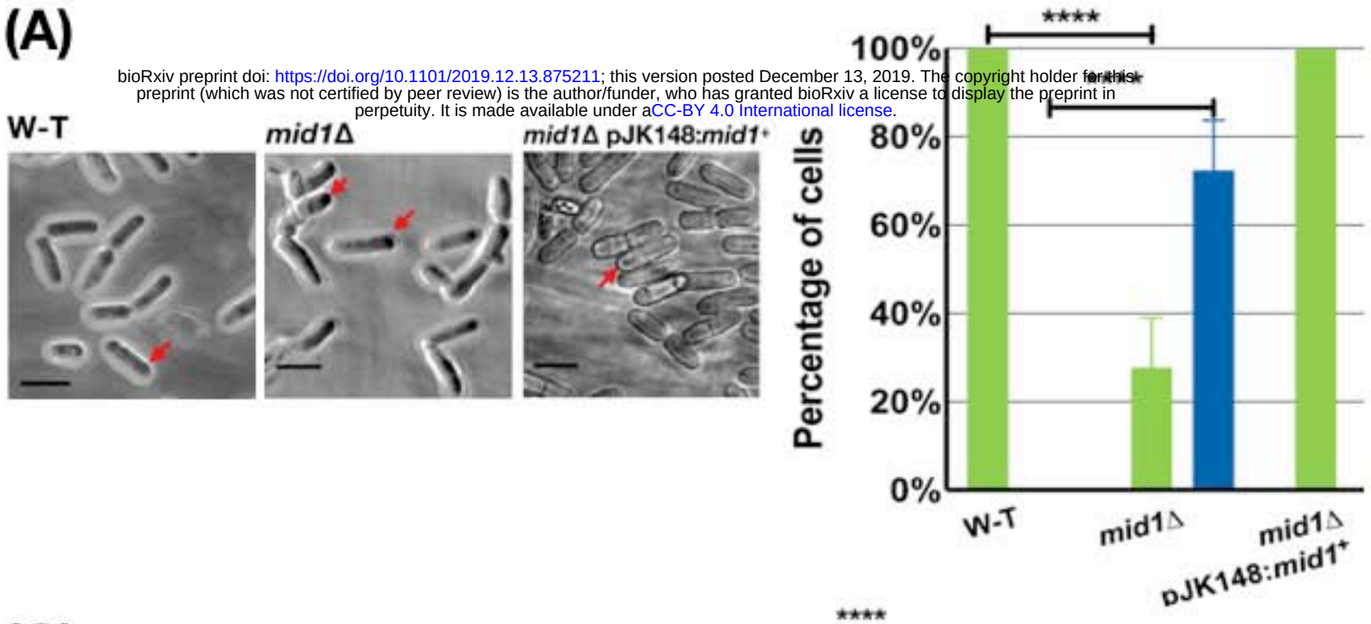

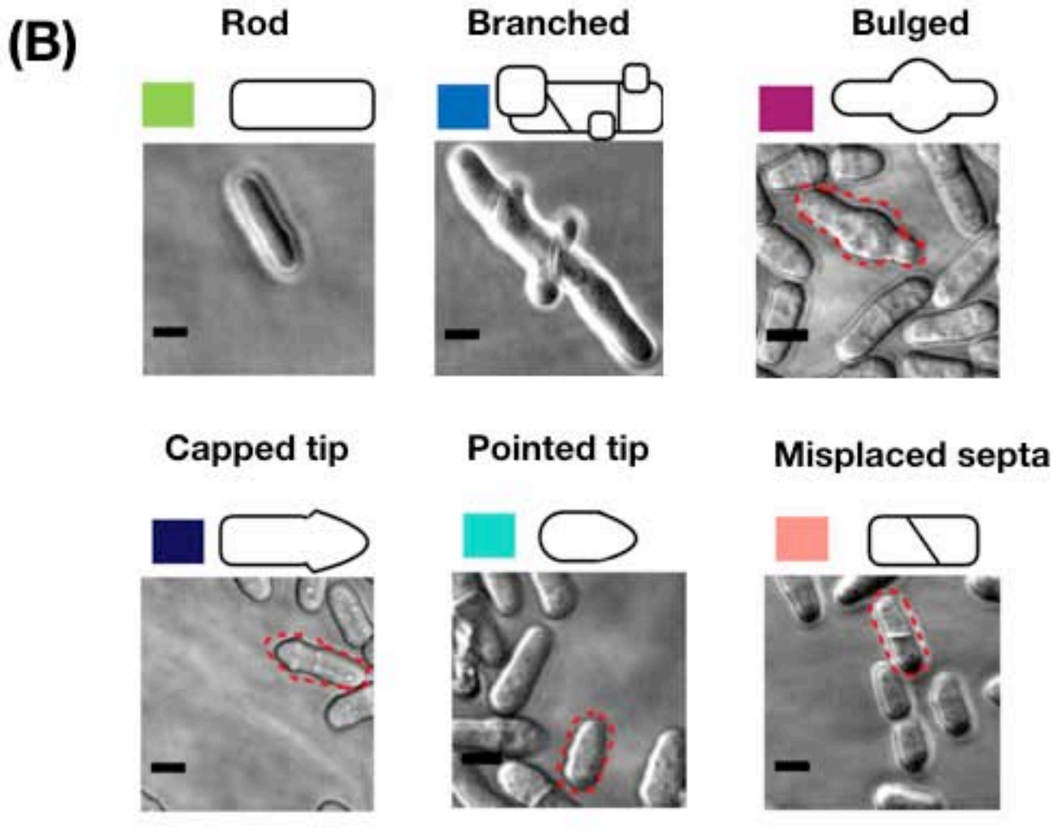

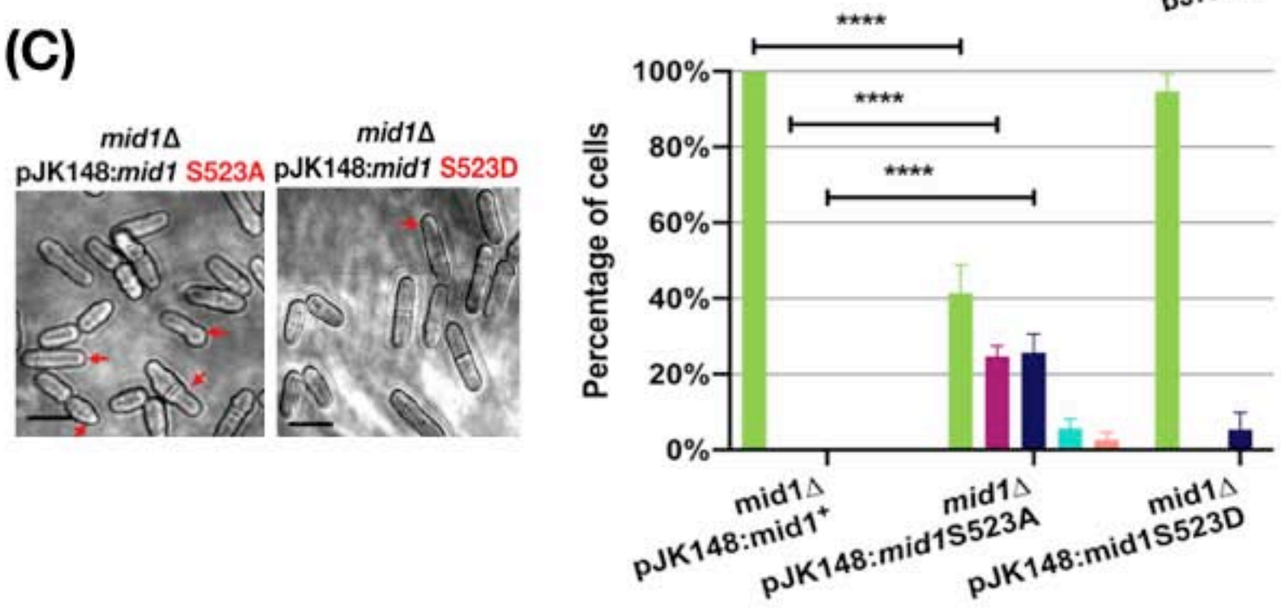

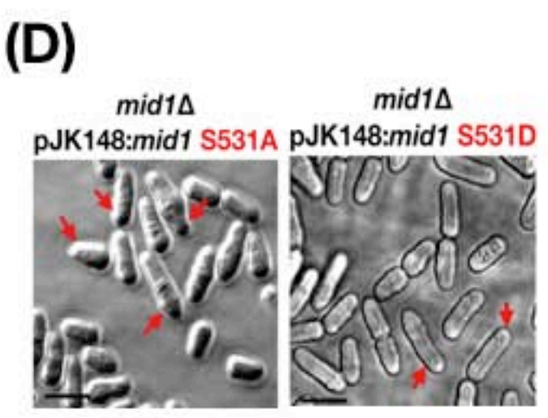

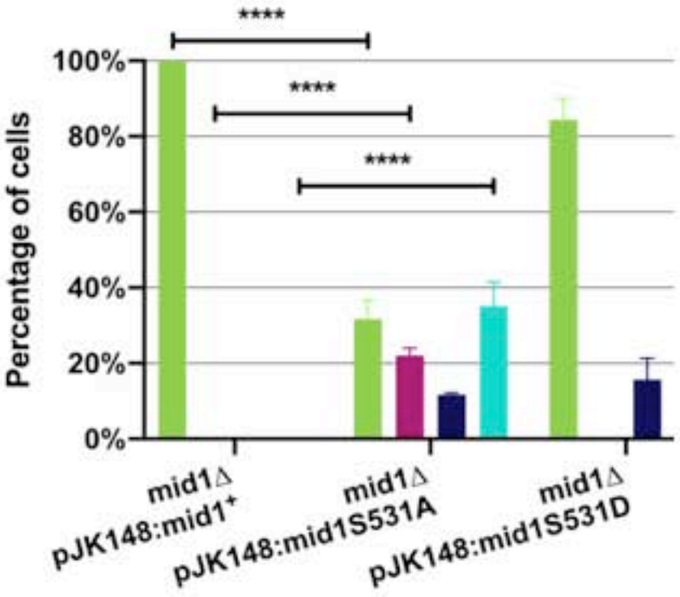

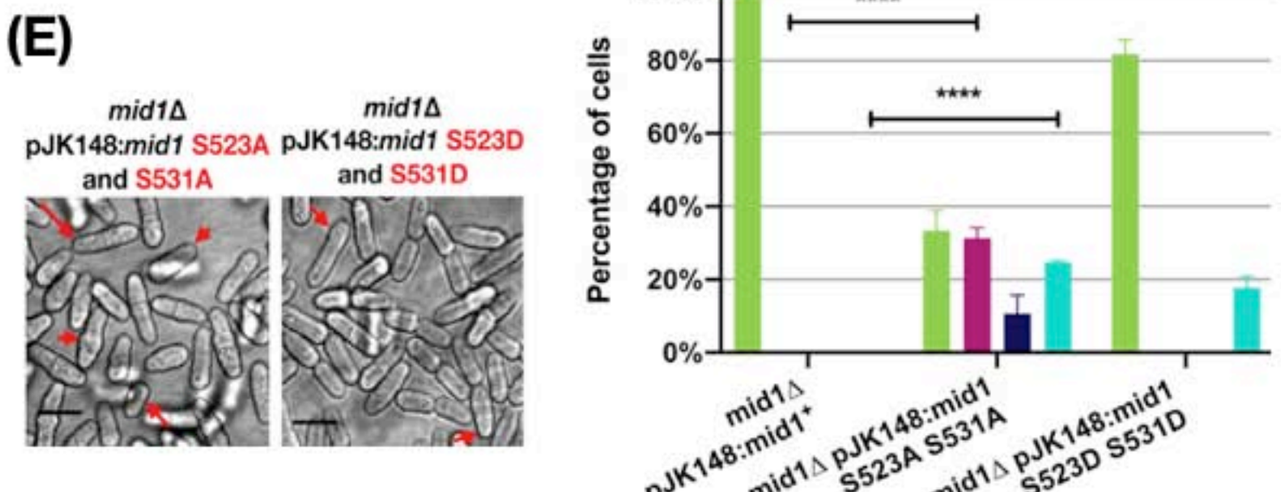

bioRxiv preprint doi: https://doi.org/10.1101/2019.12.13.875211; this version posted December 13, 2019. The copyright holder for this preprint (which was not certified by peer review) is the author/funder, who has granted bioRxiv a license to display the preprint in perpetuity. It is made available under aCC-BY 4.0 International license.

(A)

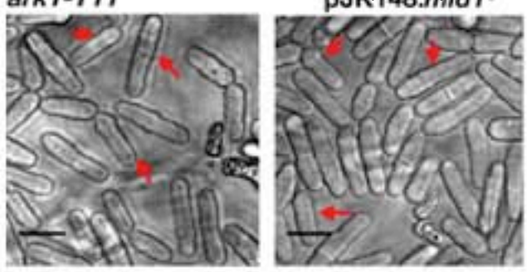

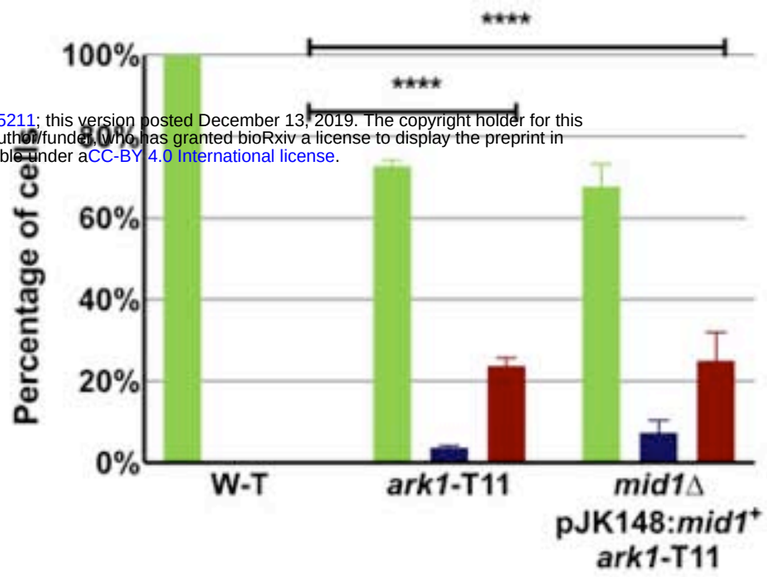

(B)

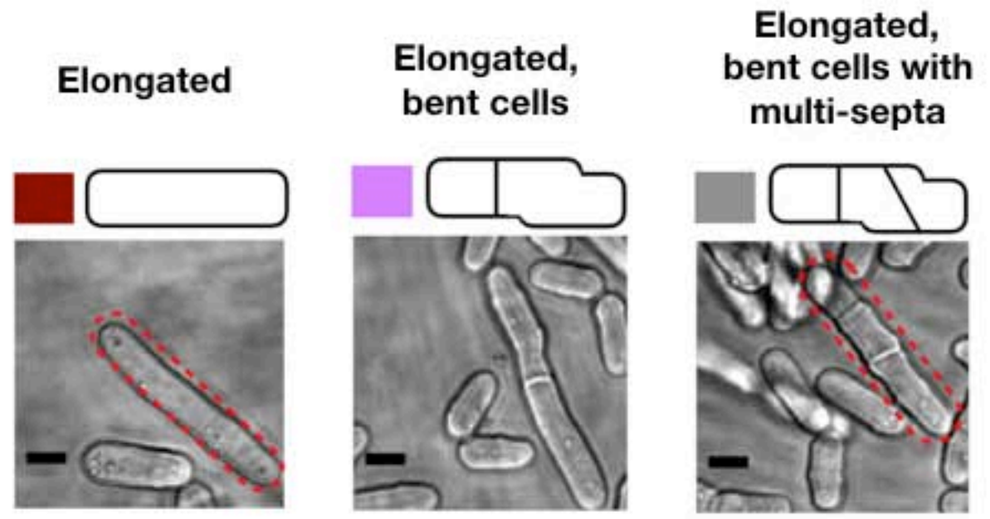

(C)

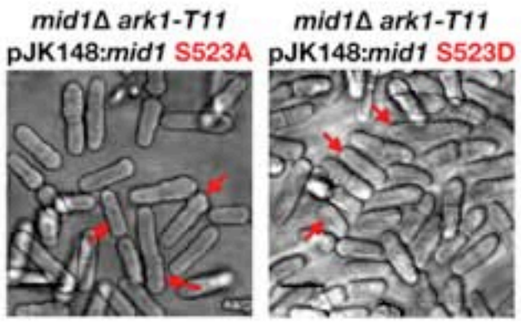

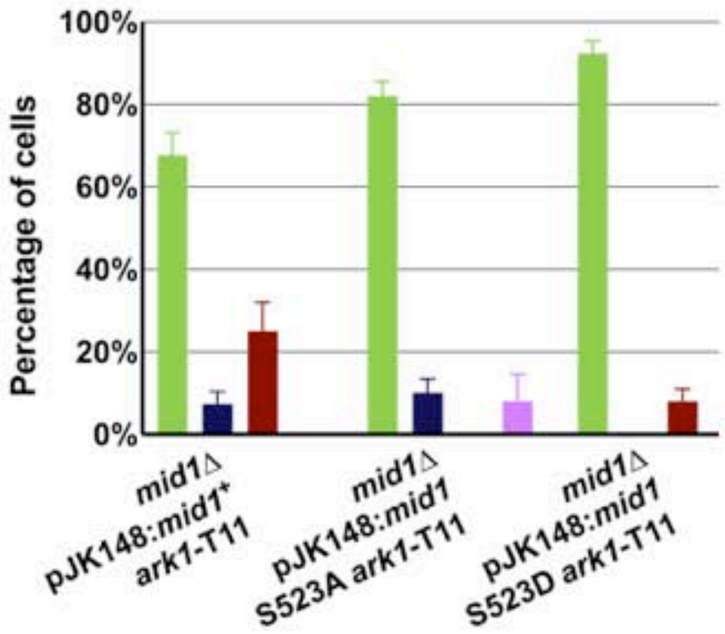

(D)

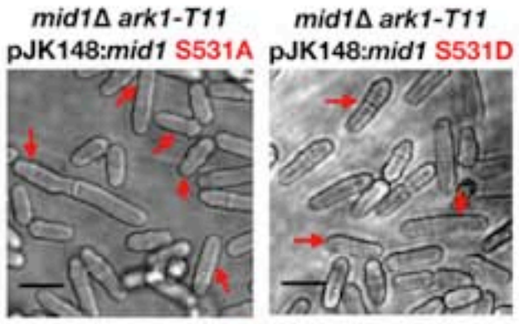

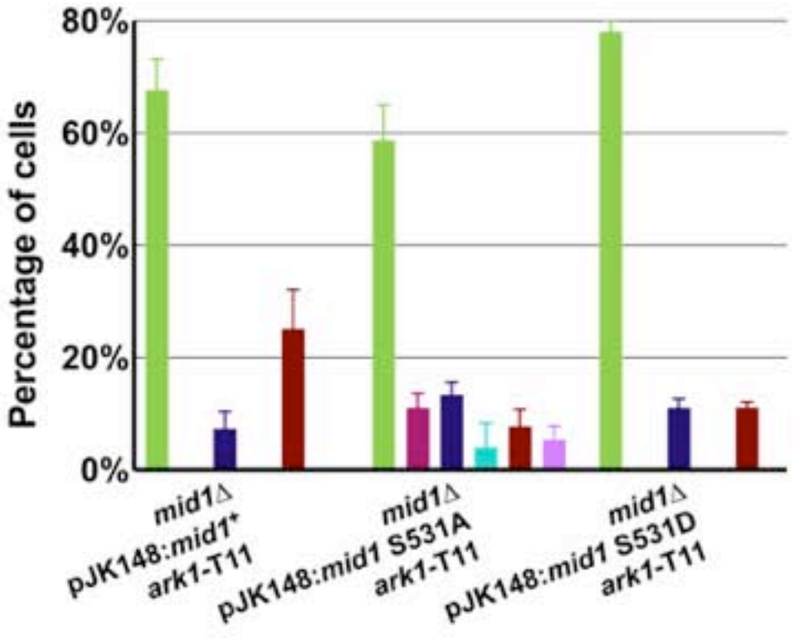
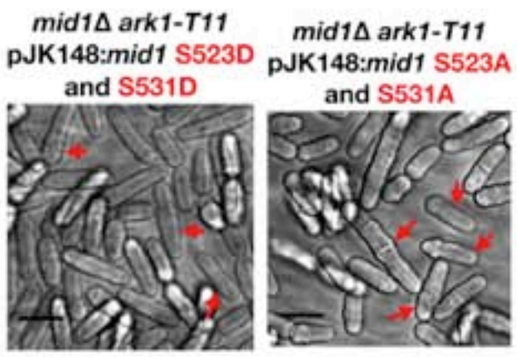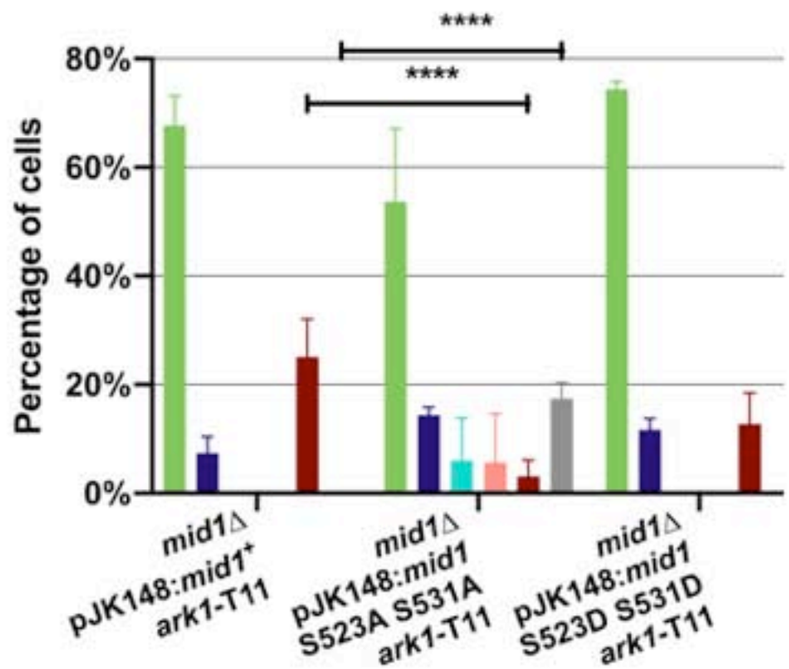
(E)